Deanship of Graduate Studies
AL-Quds University

Studying some of the Physical Properties of Matter using Eddy Current Technique

Azzam Hammed A. Abu-Sabha

M.Sc. Thesis

Jerusalem-Palestine
2005

Studying some of the Physical Properties of Matter using Eddy Current Technique

By

Azzam Hammed A. Abu-Sabha

(B.Sc. Physics, 1992, AL-Quds University, Palestine)

Supervisor: Dr. M. I. Abu - Taha

Co-Supervisor: Dr. M. M. Abu - Samreh

"A thesis Submitted to the Deanship of Graduate Studies in Partial Fulfillment of the Requirement for the Degree of Master of Physics"

AL-Quds University

Abu-Deis, Jerusalem

January, 2005

Program of Graduate Student in Physics

Deanship of Graduate Studies

Studying some of the Physical Properties of Matter using Eddy Current Technique

By:

Student Name: **Azzam Hammed A. Abu Sabha**

Registration No.: 20110943

Supervisor: Dr. M. I. Abu-Taha

Co-Supervisor: Dr. M. M. Abu-Samreh

Master thesis submitted for Examination on 6/3/2005 and accepted by the examining committee formed of the following:

Committee Members.		**Signature**
M. I. Abu-Taha, Ph.D.	(Head of committee)	----------
M. M. Abu-Samreh, Ph.D.	(Member)	----------
A. M. Saleh, Ph.D.	(Internal Examiner)	----------
J. Sulaiman, Ph.D.	(External Examiner)	----------

AL-Quds University
2005

DECLARATION

I certify that this thesis, which is submitted for the degree of master of physics, is the result of my own research, except where otherwise acknowledged, and that this thesis (or any part of the same) has not been submitted for a higher degree to any university or institution.

Signed:…….

(Azzam Hammed A. Abu-Sabha)

Date:----------

DEDICATION

To the memory of my mother

To my wonderful wife

To my beloved family

ACKNOWLEDGEMENT

It is my pleasure to express my gratitude and thanks to my supervisors Dr. M. I. Abu-Taha and Dr. M. Abu-Samreh for supervising this work. It is because of their interest, guidance, encouragement and valuable suggestions through the period of study, this work was finally accomplished.

I would like to thank my friends, Y. Al-Sarahneh A. Amaere and A. Abu-Tabekh for the unlimited assistance and encouragement. It is great pleasure to acknowledge the contribution of people in the preparation of this thesis. Special thanks will go to my daughters, Soha, Reema, Manal, Reem, and to my son Wael for their help during the preparation of this work.

Abstract

In this study, the electric and the magnetic properties of aluminum, copper, gold, mercury, and silver have been investigated using the eddy current technique. It was found that when an alternating current passes through a solenoid, only aluminum and copper rings placed in the core of the solenoid jump a few centimeters. But rings of gold, mercury and silver show no levitation at all. The levitation height was found to depend not on the ring mass and the length, but on other properties such as conductivity and density.

The calculated values for conductivity of both aluminum and copper was $(3.313 \pm 0.0721)\times10^{7}$, s/m, $(5.928 \pm 0.1461)\times10^{7}$, s/m respectively. The calculated values of relative permeability of core material was found to be 144.0, while the corresponding magnetic susceptibility is 143.0, also the specific heat of aluminum is 0.918 ± 0.0531, J/g^{0}c. The calculated values for the conductivity and the specific heat are in agreement with errors less than 8% for most measurements of the theoretical results.

الخلاصة

في هذه الدراسة، وباستخدام طريقة التيارات الدوامية تم دراسة الخواص الكهربائية والمغناطيسية للألمنيوم، والنحاس، والذهب، والزئبق، والفضة. ووجد أنه عندما يمر تيار متردد في ملف حلزوني ذو قلب معدني، وإدخال حلقة من هذه المواد حول القلب المعدني، فإن حلقات النحاس واللالمنيوم فقط هي التي ترتفع بضعة سنتمترات للأعلى. بينما حلقات الذهب، والزئبق، والفضة لم تتحرك من مكانها. لقد دلت الدراسة أن ارتفاع الحلقة لا يعتمد على كتلة الحلقة وأبعادها الهندسية مثل الطول والسمك، بينما يعتمد على خواص أخرى مثل ثابت الموصلية والكثافة. ولقد تم حساب ثابت الموصلية للألمنيوم والنحاس ووجد أنها تساوي $(3.313 \pm 0.0721)\times10^7$, s/m، $(5.928 \pm 0.1461)\times10^7$ s/m ، على التتابع، و تم قياس النفاذية المغناطيسية النسبية للقلب المعدني ووجد أنها تساوي 144.0 بينما قابلية التمغنط له تساوي 143.0، أيضاً تم حساب الحرارة النوعية للنحاس ووجد أنها تساوي، 0.918 ± 0.0531, J/g^0c ، وبشكل عام كانت النتائج التجريبية متطابقة مع النتائج النظرية بنسبة خطأ لا تتجاوز 8 % في غالبية القياسات.

Table of contents

Title	Page
Chapter One (Introduction and motivation)	1
1.1 Introduction	1
1.2 The scope of the study	7
1.3 Methodology	8
Chapter Two (Eddy current in a non-magnetic ring)	9
2.1 Introduction	9
2.2 The model	9
2.2.1 Magnetic field due to a circular current loop	10
2.2.2 The magnetic field of a solenoid	11
2.3 Induced *emf* across the floating ring	13
2.4 The eddy current produced in a metal ring	13
2.5 The levitation magnetic force on the ring	14
2.5.1 The relation between the levitation height of the ring and other variables at equilibrium	15
2.6 Applications of the model	16
2.6.1 Practical measurement of B_r and B_z	17

2.6.2 Calculation of copper conductivity using eddy current	18
2.6.3 Calculation of the number of free electrons per unit volume in copper	19
2.6.4 Calculation of density of copper using eddy current	20
2.6.5 Calculation the magnetization density of the core M	20
2.6.6 Calculation of the core permeability	21
2.6.7 Measurements of the magnetic force on the ring	21
Chapter Three (Experimental setup)	23
3.1 Introduction	23
3.2 Measurements	25
3.2.1 Measurement of B_r and B_z	27
3.2.1.1 Measurement of B_z	27
3.2.1.2 Measurement of B_r	28
3.2.2 Calculation of the conductivity density and number of free electrons per unit volume in copper	30
3.2.3 Measurements of the magnetization density permeability of the core and the lowest current needed to rise the temperature of the ring	30
3.2.4 Measurement of the induced potential across two opposite points on the ring	31
Chapter Four (Results and discussion)	33
4.1 Introduction	33

4.2 Results	33
4.3 Results of ring levitation	34
4.3.1 Results of magnetic fields	34
4.3.2 Results of levitation force	39
4.3.3 Results of ring levitation	41
4.3.3.1 Ring levitation dependence on its length	41
4.3.3.2 Ring levitation dependence on its thickness	43
4.3.3.3 Ring levitation dependence on thickness and length	44
4.3.4 Induced potential across two opposite points on the ring	56
4.3.5 The effect of cracks on the eddy current	58
4.3.6 Investigations of special non-magnetic rings	61
4.4 Applications to eddy current measurements	62
4.4.1 Calculation of the conductivity	62
4.4.2 Calculation of the specific heat	63
4.4.3 Calculations of the number of free electrons per unit volume and the mean time between electron collisions	66
4.4.4 Calculation of magnetization density M and the magnetic field intensity H	67
4.4.5 Calculation of the relative permeability μ_r	68
4.4.6 Calculation of the magnetic susceptibility χ	70
4.4.7 Calculation of the eddy current induced in the ring	70
4.4.7.1 Calculation of the eddy current using the heat	71

dissipation method	
4.4.7.2 Calculation of the eddy current by measuring *emf*	73
4.4.7.3 Dependence of ring temperature on time	73
4.5 The effect of ring dimension on the current drawn by the solenoid	74
4.6 The levitating solenoid	76
Chapter Five (Conclusions and further work)	78
Appendix A	82
Appendix B	93
References	118

Figure Caption

Figure No.	Figure	Page
Figure 1.1	Schematic representations of the circulation of electrons in a conductive ring in the presence of an external magnetic field B.	1
Figure 2.1	Schematic representations showing the resultant radial forces on the ring F_r.	15
Figure 2.2	Schematic representations showing a coil winded around the metal core through the solenoid. to measure the field in the core.	18
Figure 2.3	Schematic representations showing, (a) The solenoid and the non-conducting rings. (b) Non-conducting rings added on the top of levitated ring to measure the force on the ring.	22
Figure 3.1	Schematic representations showing the jumping ring complete apparatus.	25
Figure 3.2	Schematic representations showing a coil winded around the metal core through the solenoid used to measure the field in the core.	28
Figure 3.3	Schematic representations showing the apparatus needed to measure the radial component of magnetic field, B_r, from point near the core (1).	29
Figure 3.4	Schematic representations showing the apparatus needed to measure the radial component of magnetic field, B_r, from point near the core (2).	29

Figure 3.5	Schematic representations showing the apparatus needed to measure the eddy current in the ring.	31
Figure 3.6	Schematic representations showing the apparatus that used to measure the induced *emf* across two opposite points on the ring with longitudinal crack (closed circuit).	32
Figure 3.7	Schematic representations showing the apparatus that used to measure the induced *emf* across two opposite points on the ring with longitudinal crack (open circuit).	32
Figure 4.1	Dependence of the vertical magnetic field B_z at the end of the solenoid with core on the current in the solenoid.	34
Figure 4.2	Variation of the B_z with the levitation height.	35
Figure 4.3	Dependence of B_r at the end of the solenoid on the current through it.	36
Figure 4.4	Variation of B_r with the radial distance r measured from center.	37
Figure 4.5	Variation of B_r with radial distance r measured from point near the core.	38
Figure 4.6	Schematic representations showing the field lines of a circular loop and the orientation of B_r.	39
Figure 4.7	The dependence of the force acting on the ring on the current passing in the solenoid for low current regions.	40
Figure 4.8	The dependence of the force acting on the ring on the current passing in the solenoid for high current regions (3-10) A.	40
Figure 4.9	Levitation height versus the ring length for different input currents.	42

Figure 4.10	Levitation height of the lower end of copper ring versus its length for fixed current.	42
Figure 4.11	Schematic representations showing the effect of gravitational torque on large radius ring.	43
Figure 4.12	The relation between levitation height of different thickness for yellow brass rings, when having a diameter of 4 mm and for a fixed input current.	44
Figure 4.13	Schematic representations of (a) the random direction of the dipole moments in material. (b) the alignment of dipole moments in material when it is placed in an external magnetic field.	46
Figure 4.14	Schematic representations showing the interaction between two dipole moments.	49
Figure 4.15	Relation between F(z) and z at constant applied current 2 A.	53
Figure 4.16	Schematic representations showing the portion of the ring affected by the force.	54
Figure 4.17	Levitation height dependence on length.	55
Figure 4.18	Schematic representations showing different cracks that can be introduced to the ring.	58
Figure 4.19	Dependence of the length of longitudinal downward crack in the ring and the corresponding levitation height as current is swept over the range 0.5-4 A, one curve to a crack.	59
Figure 4.20	Schematic representations showing the circulation of eddy current in the ring with two kinds of cracks (a) longitudinal cracks. (b) latitudinal cracks.	60

Figure 4.21	Relation between E_1 and E_2, parameter needed to calculate the specific heat capacity.	66
Figure 4.22	Relation between the magnetization density M and the magnetic field intensity H for metal core.	67
Figure 4.23	Relation between the relative permeability of the core versus the current in the solenoid.	70
Figure 4.24	Relation between the temperature of copper ring versus time.	74
Figure 4.25	The relation between the current in the solenoid coil and the thickness of aluminum ring for fixed rings length.	75
Figure 4.26	The relation between the current in the solenoid coil and the length of copper ring for fixed rings thickness.	75
Figure 4.27	Schematic representations showing the extended magnetization area inside the ellipsoids for two currents i_1 and i_2 such that $i_2 > i_1$.	77
Figure B.1	The magnetic field produced by circular current loop carrying a current I at space point P.	93
Figure B.2	Schematic representations of the magnetic field due to circular current loop carrying a current I at P (x,0,z).	98
Figure B.3	Schematic representations of the two components B_z and B_r of the magnetic field B due to a circular current loop.	99
Figure B.4	Schematic representations showing a solenoid of N turns and the point P along solenoid axis where the magnetic fields should be calculated.	101
Figure B.5	Schematic representations of the ring dimensions and the flow of the eddy current through it.	107

Figure B.6	Schematic representations showing measurement arrangement of the induced *emf* across the ring between two points.	108
Figure B.7	The magnetic field B through copper ring of cross sectional area A.	109
Figure B.8	The vertical force on the ring F_z.	112
Figure B.9	Schematic representations showing the resultant radial forces on the ring F_r.	113
Figure B.10	Elevation of copper ring above a solenoid coil carrying AC current.	115

List of tables

Table No	Table	Page
Table A.1	Data of the magnetic field B_z at the end of the solenoid and the current in the solenoid.	82
Table A.2	Data of the magnetic field B_z of the solenoid with core versus levitation height z over the top of the solenoid at constant current of (3 A).	82
Table A.3	Data of the magnetic field B_r at the end of the solenoid directly above the first turn and the current passing through the solenoid.	83
Table A.4	Data of the magnetic field B_r at the end of the solenoid and the radial distance r at constant input solenoid current of 1 A.	83
Table A.5	Data of B_r and the radial distance from the core r measured at the top of the solenoid for constant solenoid current of 2 A.	84
Table A.6	The induced *emf*, the current, the magnetic field, belong to a copper ring rests at the end of the solenoid for 20 mm ring length.	84
Table A.7 a	The dependence of the center of mass levitation height on the length of copper ring at different applied currents.	85
Table A.7 b	The dependence of levitation height of a copper ring on length (for a long ring) at an applied current of 2.2 A.	85

Table A.8	Thickness, length and outer diameter of various rings of yellow copper.	86
Table A.9	The levitation height, the thickness of yellow copper rings for two different currents in the solenoid at fixed interior radius (r_1).	86
Table A.10	The induced *emf* across copper and aluminum rings having 0.77 mm thickness and 11 cm long for different heights along the ring, when the potential across the solenoid coil 30 V.	86
Table A.11	Crack properties, the current in the solenoid and the corresponding levitation heights for aluminum ring of 26 mm long.	87
Table A.12	Parameters of gold, silver and mercury when used in levitation ring experiment.	88
Table A.13	The variable parameters for both aluminum and copper rings (needed to calculate the conductivity).	88
Table A .14	Measured data used to calculate the specific heat capacity of aluminum, when the voltage across the solenoid coil 12.3 V and the initial temperature of the ring (T_i) 25 ^{0}C.	89
Table A. 15	The relation between the magnetic field B_z at the end of the solenoid with core and the current in the solenoid.	89
Table A.16	The magnetization density, M, over the end of the solenoid and the current in the solenoid at point on the core 0.4 cm above the upper end of the solenoid.	90
Table A.17	The induced *emf* and other properties of aluminum, copper and metal rings.	90
Table A.18	The current drawn by the solenoid coil and the thickness of aluminum ring, for fixed rings length of 9.5 mm and potential across the solenoid coil 20 V.	91

Table A.19	The drawn current by the solenoid coil and the length of copper ring, for fixed rings thickness 0.77 mm and potential difference of 20 V.	91
Table A.20	The B_r and the corresponding radial distance from the core (r) measured at the top of the solenoid for constant solenoid current of 2 A.	91
Table A.21	The fluctuations and the systematic errors of apparatus.	92

Chapter One

Introduction and motivation

1.1 Introduction

The magnetic properties of matter are the result of microscopic atomic currents, which produce magnetic moments in matter (Kip, 1969; Page and Adams, 1987; Taylor, 1988). The discussion here is limited to those materials, in which an external field induces magnetic moments (conductive materials). In materials, the magnetic distribution inside matter is proportional to the applied external field. If the specimen material is isotropic, an external field induces magnetic dipoles which on the average, are aligned with their moment along the direction of the applied field as displayed in Figure 1.1. The effect of such alignment is known as magnetization of mater (Hammond, 1971; Aiello and Alfonzetti, 2000).

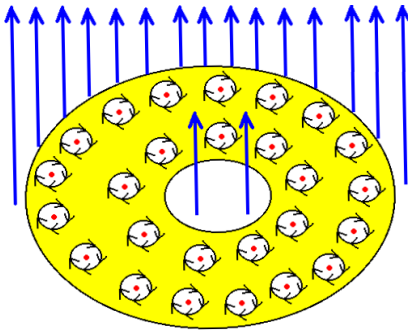

Figure 1.1 Schematic representations of the circulation of electrons in a conductive ring in the presence of an external magnetic field B.

However, the presence of an external magnetic field causes the atomic electrons to move in a direction perpendicular to applied fields. The magnetic properties of the substance depend on the manner of electron rotations especially its spinning. Accordingly, every rotation can be considered as a circular current loop around which a magnetic field is produced. When a conducting substance is subjected to alternating magnetic field, electrons rotation opposes the applied magnetic field (Lenz's law). Consequently, an alternating current known as an eddy current is produced (Hallidy *et al.*, 2001; Thompson, 1990).

An eddy current is that current produced inside a substance, when placed in alternating magnetic field, or when magnetic field gradient are switched on (Deene *et al.*, 1999; Aiello and Alfonzetti, 2000). Its origin goes back to Michael Faraday's discovery of electromagnetic induction in 1831. In 1879, another scientist named Hughes had recorded some changes in the properties of a coil when placed in contact with metals of different conductivity and permeability. However, it was not until the Second World War that these effects were put to practical use for testing materials. Much work was done in the 1950's and 60's, particularly in the aircraft and nuclear industries.

An eddy current has so many effects on materials among which, heating of substances and causing objects to move. Besides, some of the physical properties of materials can be studied using the so called eddy current technique. This type of current depends mainly on the physical properties of the substance (Portis, 1978). Therefore, the effects of alternating magnetic fields on the materials and the eddy current strengths that produce such fields were used to investigate the physical properties of substances.

The eddy current testing is now widely used as a well-established inspection technique (Gros, 1995; Lebrun *et al.*, 1997; Bishop, 2001). This type of testing is used for inspection of conductive materials by inducing electrical currents in the test material and recording any variations of the induced currents. A basic eddy current system usually consists of a coil, which is excited by an alternating current. The electric current within the coil creates a primary magnetic field, B, surrounding the coil. When such field is brought into the proximity of the test material, the primary electromagnetic field induces eddy current in the tested material. According to Lenz's law, eddy currents themselves generate a secondary magnetic field, B, opposes to the primary magnetic field (Gros, 1995). Thus far many applications of eddy current technique had been invented. For instance,

Freeman used the eddy current technique to study the equivalent circuit of concentric cylindrical conductors in an axial alternating magnetic field (Freeman *et al.*, 1975; Freeman and Bland, 1976). The second application was the detection of damage caused by low-energy impacts on carbon fiber reinforced materials (Gros, 1995). The third application is the description of eddy current stream lines within a conducting slab of a non-magnetic material when crossing, with a constant velocity, and a permanent magnetic field (Restivo, 1996). Rao and Babu in 1996, had studied the simulation of eddy current signals from multiple defects (Rao and Babu, 1996). Moreover, this technique can be used to detect the deep defects in conductive materials (Lebrun *et al.*, 1997). The eddy current microscopy was studied by Hoffmann (Hoffmann *et al*., 1997). Sikora and Komorowski used this technique to determine the conductivity and the permittivity of materials (Sikora *et al*., 2000). The assessment of eddy current sensitivity and correction in single-shot diffusion-weighted imaging was studied by Koch (Koch and Norris, 2000).

The Influence of eddy currents on magnetic hysteresis loops in soft magnetic materials had been investigated by Szczyglowski (Szczyglowski, 2000). The eddy current can be used to study the temperature dependent permeability (Cimatti, 2003). The eddy current theory and its applications in

different areas were investigated in details by many research groups (Gros, 1995; Lebrun *et al.*, 1997; Hoffman *et al*., 1997).

The jumping ring experiment is one of the most important experiments used to study the eddy current (Summner and Thakkrar, 1972; Hall, 1997). It was invented in the last century by an American, Elihu Thomson, and sometimes it is referred to as 'Thomson's ring' (Ford and Sullivan, 1991). Hundred years ago, Fleming who later discovered the thermo ionic diode, described in some details various experiments with the jumping ring apparatus (Fleming, 1970).

Summner and Thakkrar (1972) had studied the jumping ring experiment, and found that both the vertical B_z and radial B_r components of the magnetic field of the solenoid, decrease approximately linearly with levitation height. Besides, the force acting on the ring was found to be proportional to B_rB_z.. At equilibrium, the force become equal to the weight of the ring, and therefore B_rB_z = constant. It was found that the levitation height to which the ring levitates is independent of the thickness of the ring in the range (2-4) mm (Ford *et al.*, 1992).

When a non-magnetic conducting ring inserted in the metal core of a solenoid, and an AC current is allowed to pass through the solenoid coil, the magnetic forces cause the ring to jump up several centimeters (Restivo,

1996; Avrin, 2000). Hall in 1997 had been investigated the relation between the force on the ring and the amplitude and frequency of current supplied to the solenoid (Hall, 1997). His investigation has shown that the force on the ring varies as the square of the current passing through the solenoid and on the frequency of the source current. On one hand, investigating such phenomenon, the relation between the eddy current induced in the ring and its density, resistance, conductivity…. etc, will be possible. On the other hand, the size of the eddy current and its dependence on ring shape, current in the solenoid, and type of material, were also of special interest. Accordingly, brass, aluminum, mercury, and silver are among several materials that can be tested. In addition, testing the effect of cracks and bores in the ring were also included. In this work, the main aim is to investigate experimentally the relations among the above factors and to develop a theoretical model good enough to explain the experimental observations.

1.2 The scope of the study

In this study, some properties of materials will be addressed using eddy current induced in a non-magnetic conducting ring placed in alternating magnetic field, (i.e. the jumping ring). When such a ring is inserted in the metal core of a solenoid, in which an alternating current is passed through, magnetic forces resulted from the eddy current in the ring will cause the ring to jump up to several centimeters (Restivo, 1996; Avrin, 2000). Investigating such phenomenon is expected to explore some relations between the eddy current induced in the ring and its density, magnetic permeability, conductivity…. etc. Moreover, the size of the eddy current and its dependence on ring shape, current supplied in the solenoid and type of material are also of special interest.

Theoretically, the main aim of this study is to derive relations between eddy currents produced in the non-magnetic materials when immersed in an alternating magnetic field and some electrical parameters as well as to examine some characteristics of the material. Besides, electric and magnetic properties and parameters of some conducting materials (conductivity, permeability, magnetization density, matter density, and the number of conducting electrons per unit volume) will be studied using eddy current

technique. Investigating such properties will require designing devices that can be used to measure and test such properties easily.

1.3 Methodology

If a non-magnetic conducting ring is inserted in the metal core of a solenoid, which carries an alternating current, then an eddy current will flow in the ring causing it to levitate up several centimeters (Avrin, 2000; Restivo, 1996). The amount of levitation height depends mainly on the eddy current induced in the ring which in turn depends on several properties of the ring material. The study of these properties theoretically and experimentally requires a full study of the eddy current induced in conducting non-magnetic materials. This requires developing a model that meets all the variances of the current and the ring material.

It turns out that for iron and its alloys or other transition element alloys such as Co, Ni, Gd, and Dy, a special effect occurs. Such effect permits a specimen to achieve a high degree of magnetic alignment in spite of the randomizing tendency of the thermal motions of the atoms.

Chapter Two

Eddy current in a non-magnetic ring

2.1 Introduction

An eddy current is that current produced inside a substance when placed in an alternating magnetic field (Auld and Moulder, 1998). It has many effects on materials such as, heating of substance and it may cause them to move. In this chapter, we shall develop a model capable on producing the dependence of electric and magnetic properties on eddy currents. The rest of this chapter deals with the theoretical derivations of certain physical parameters such as conductivity, susceptibility – etc., required to understand the technique and its possible uses in the best way (Barth, 2000; Thong and Fenglie, 2002).

2.2 The model

In order to investigate the effect of the eddy current on a levitating ring theoretically, a model has to be developed. When a non-magnetic metal ring is inserted in the metal core pivoted in a solenoid through which an alternating current is passing, an eddy current is produced in the ring as shown in Figure 1.1 (Restivo, 1996; Avrin, 2000; Huang, 2003). This current induces a magnetic field in the vicinity of the ring. The two magnetic fields (the field produced by the solenoid and that of the ring) are

acting in opposite directions (Freeman and Lother, 1989; Freeman, 1992; William, 2000). As a result of the repulsive force between the magnetic field produced by one solenoid and the opposing one induced by the eddy current in the ring, the ring will levitate (Portis, 1978; Blitz and Alagoa, 1985; Restivo, 1996; Avrin, 2000). The equilibrium point is found to depend on the properties of the non-magnetic metal ring.

The ring reaches the equilibrium point when the weight of the ring equals to the repulsive force. Thus, an expression for the magnetic force acting on the ring to bring it to equilibrium point is of great importance**.** In order to study such force, an expression for the magnetic field (B) produced inside the solenoid at any point near the core is required. To derive such a field, the magnetic field due to a circular current loop will be derived, and then this field will be integrated over all the turns of the solenoid.

2.2.1 Magnetic field due to a circular current loop

The magnetic field at point P in the vicinity of a circular current loop of radius a can be written in a vector form as (Appendix B):

$$\vec{B} = B_r \vec{r} + B_z \vec{z} \qquad (2.1)$$

Where B_r and B_z are the radial and the vertical component of the magnetic field $\vec{B}$ at P. According to Appendix B, these components can be written as:

$$B_r = \frac{3\mu_0 I a^2 R^2 z' r}{4\pi\left(a^2 + z'^2\right)^{5/2}} \tag{2.2}$$

and

$$B_z = \frac{\mu_0 I a^2}{2(a^2 + z'^2)^{3/2}} \tag{2.3}$$

2.2.2 The magnetic field of a solenoid

Similarly, the magnetic field components (the radial and the vertical) at point P near a solenoid of N turns and length L can be represented by (see appendix B):

$$B_z = \frac{\mu\ NI_0}{2L}\left[\frac{(z+L)}{f} - \frac{z}{y}\right]\sin(\omega t) \tag{2.4}$$

$$B_r = \frac{Na^2\mu_0 Ir}{4}\left[\frac{f^3 - y^3}{f^3 y^3}\right]\sin(\omega t) \tag{2.5}$$

Where the parameters *y* and *f* are given by:

$$y = \sqrt{\left(a^2 + z^2\right)} \tag{2.6}$$

and

$$f = \sqrt{\left(a^2 + (z+L)^2\right)} \tag{2.7}$$

The rest of the symbols appeared in equation (2.4) and equation (2.5) can be introduced as:

N is the number of turns of the solenoid coil,

a is the radius of the cross section of the solenoid coil,

I_o is the current in the solenoid,

L is the solenoid length,

z is the levitation height of the point P over the edge of the coil,

r is the radial distance from the core to P.

The magnetic field inside the core, B_{in}, can be written as:

$$B_{in} = B_{ext} + \mu_o M = B_{ext} + C_3 \qquad (2.8)$$

Where B_{ext} is the external magnetic field produced by the solenoid, C_3 is constant (= μ_o M), M is the magnetization density of the metal core and μ_o is the permeability of the air. Therefore, by making use of equation (2.4) and equation (2.5), we get

$$B_{z\ in} = \frac{\mu_o I_o}{2L}\left[\frac{z}{y} - \frac{(z+L)}{f}\right] + C_3, \quad \text{for } r > \text{a} \qquad (2.9)$$

and

$$B_r = \frac{Na^2 \mu_0 Ir}{4}\left[\frac{f^3 - y^3}{f^3 y^3}\right], \quad \text{for } 0 \le \text{r} \le \text{a} \qquad (2.10)$$

2.3 Induced *emf* across the floating ring

Let a non-magnetic metal ring is inserted in the metal core of a solenoid and allowing an alternating current to pass through. An *emf* will be produced across the ring as a result of the electromagnetic induction of the z component of the alternating magnetic field B_z. It can be shown that the maximum *emf* can be written as (see appendix B):

$$emf_{\max} = \omega\, B_{z0} A = \omega\, B_{z0}\, \pi x^2 \qquad (2.11)$$

The *emf* is the induced voltage across the terminals of the open circuit ring, x is the radius of the core, B_{zo} is the maximum vertical magnetic field at the center of the ring, and ω is the angular frequency of the power supply. Accordingly, the induced *emf* is independent on the area of the ring but it depend on the cross sectional area of the core. This is because all field lines were inside the core.

2.4 The eddy current produced in a metal ring

If the ring is considered as a complete short circuit, the *emf* produced across the ring as a result of the induced eddy current, *dI*, circulating in the ring was found to be written as (see appendix B):

$$I = \frac{\omega A t B_{z0} \sigma\ L}{l} \qquad (2.12)$$

where σ is the conductivity of the ring, and l is the circumference of the ring.

2.5 The levitation magnetic force on the ring

The force acting on the ring can be obtained simply by performing the following cross product:

$$d\vec{F} = id\vec{l} \times \vec{B} \tag{2.13}$$

Since the magnetic field has two components, namely B_r and B_z, the ring is expected to be subjected to two different forces. The first one is the vertical component F_z, which arises from the interaction of B_r with the induced field from the eddy current in the ring. The second one is the result of interaction of B_z with the induced field from the eddy current in the ring. Such force represents the radial component of the resultant force, F_r, and is directed along the r direction. Because of symmetry, the resultant of F_r is zero (see Figure 2.1) (Summner and Thakkrar, 1972). It can be shown that the vertical component of the magnetic force on the ring F_z, is defined accordingly (see Appendix B):

$$F_z = \int_{z_1}^{z_2} \left[\omega\, tA\sigma \frac{N^2 a^2 \mu_0{}^2 i^2 r}{8L} \left[\frac{z}{y} - \frac{(z+L)}{f} \right] \left[\frac{f^3 - y^3}{f^3 y^3} \right] \right] dz \tag{2.14}$$

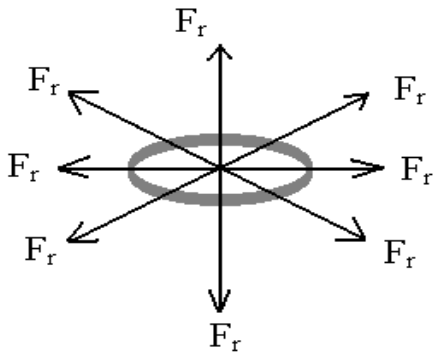

Figure 2.1 Schematic representations showing the resultant radial forces on the ring F_r.

2.5.1 The relation between the levitation height of the ring and other variables at equilibrium

The ring levitates few centimeters before it reaches the equilibrium position where the magnetic force on the ring should be equal to its weight (Ford and Sullivan, 1991). If this condition is met, then by integrating equation (2.14) and equating the obtained expression by the rings weight, an expression for the electrical conductivity of the ring can be written as (see appendix B):

$$\sigma = \frac{\rho}{\frac{\omega x^2}{2g}\left(\frac{\mu_0 N i_0}{2L}\left[\frac{(z+L)}{f} - \frac{z}{y}\right] + C_3\right)\left(\frac{Na^2 \mu_0 i_0}{4}\left[\frac{f^3 - y^3}{f^3 y^3}\right]\right)} \qquad (2.15)$$

where ρ is the density of the ring.

By making use of equation (2.15), other properties such as, the mobility ($\boldsymbol{\mu}$), the mean free time (τ), the number of conducting electrons per unit volume (n), carrier mean free path (λ), the drift velocity (υ_d), the current density (J), the susceptibility (χ), and the permeability (μ) can be derived. Expressions for all mentioned parameters are summarized by the following equations:

$$\text{current density } J = Nev_{drift} \tag{2.16}$$

$$\text{conductivity } \sigma = \frac{Ne^2\tau}{m_e} \tag{2.17}$$

$$\text{mobility } \mu = \frac{e\tau}{m_e} \tag{2.18}$$

$$\text{mean free path } \lambda = 2\tau v_{thermal} \tag{2.19}$$

$$\text{magnetic susceptibilty } \chi = \frac{\mathrm{M}}{H} \tag{2.20}$$

$$\text{permeability } \mu = \mu_0(1+\chi) \tag{2.21}$$

Where H is the magnetic field intensity and m_e is the electron mass.

2.6 Applications of the model

Equation (2.15) is a very important one, because it contains so many interesting properties of the material, such as: conductivity, permeability, density, magnetization density and the demagnetization factor. All these properties can be calculated from the parameters in equation (2.15). This is

the scope of Chapter 3. Furthermore, by making use of relations between these properties and other magnetic and electric properties such as the magnetic susceptibility χ, the mean free path λ, the current density J, etc., can be calculated. Therefore, this enhances the eddy current technique for investigating the levitating of a ring of certain metal as an alternative approach for studying the non-magnetic characteristics of materials.

2.6.1 Practical measurement of B_r and B_z

In this experiment, we need to measure B_z inside the core using a teslameter. Since the probe of the teslameter can not be inserted inside the core, another technique has been employed. The general trend of this technique is as follows: firstly, the induced voltage, *emf*, across the n turns of copper wire of crosses sectional area, A, winded around the core, and placed in the region of interest (where measurement of B_Z is required) should be measured. Secondly, by using Faraday's law of induction, B_Z can be calculated. Thirdly, the B_r component can be measured by setting the turns (horizontally) in the region of interest to measure B_r (see Figure 2.2), (Summner and Thakkrar, 1972). If the area of the secondary coil and the frequency of the driving AC current are chosen to be constant and the number of turns n is chosen to be $\frac{1}{A\omega}$, equation (2.11) becomes

$$B_{zo} = emf_{\max} \tag{2.22}$$

In this case, B_z is just equal to the direct reading of the voltmeter connected to the coil as displayed in Figure 2.2.

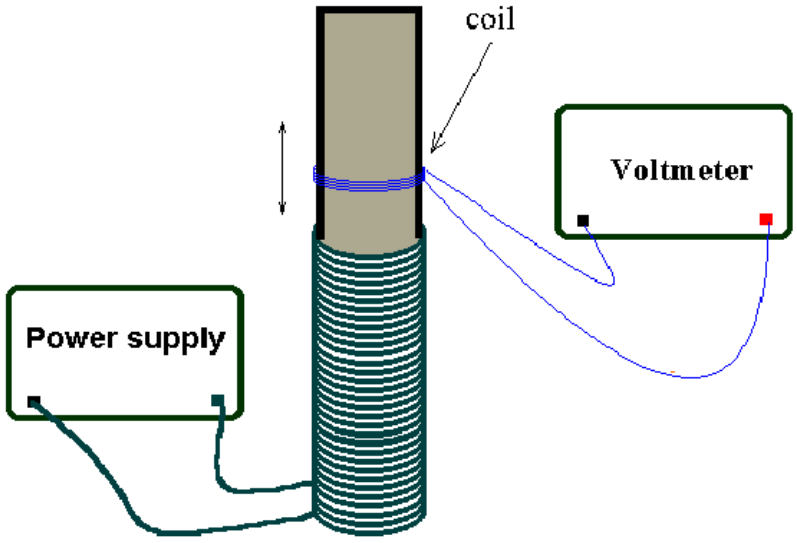

Figure 2.2 Schematic representations showing a coil winded around the metal core through the solenoid to measure the field in the core.

2.6.2 Calculation of copper conductivity using eddy current

In order to calculate the conductivity of the ring material using the jumping ring experiment, an annulus ring can be inserted around the core passing through a solenoid in which a current can be raised slowly until the ring levitates several centimeters. Then the copper conductivity can be

calculated by making use of equation (2.15). In general, the conductivity dependence on frequency is given by (Portis, 1978):

$$\sigma = \frac{\sigma_0}{\left(1+(\omega\,\tau)^2\right)^{1/2}} \tag{2.23}$$

where σ_0 is the conductivity at zero frequency, or the case when direct current is applicable. Since the mean time τ between collisions of electrons in copper is in the order of 10^{-14} s and the frequency is 50 Hz, equation (2.23) can be approximately to

$$\sigma = \sigma_0 \tag{2.24}$$

2.6.3 Calculation of number of free electrons per unit volume in copper

From the relation between the conductivity and the number of free electrons, the number of free electron in copper can be written as (Kip, 1969):

$$\sigma = \frac{Ne^2}{m_e}\tau \tag{2.25}$$

Substituting equation (2.25) into equation (2.15) to get:

$$n = \frac{\rho}{\frac{\omega\,\tau\,\sigma\,e^2x^2}{2gm_e}\left(\frac{\mu_0 NI_0}{2L}\left[\frac{(z+L)}{f}-\frac{z}{y}\right]+c_3\right)\left(\frac{Na^2\mu_0 I_0}{4}\left[\frac{f^3-y^3}{f^3y^3}\right]\right)} \tag{2.26}$$

where n is the number of free electron per unit volume, e is the electron charge and m_e is the electron mass.

2.6.4 Calculations of the density of copper using eddy current

Consider a small ring of 2 mm long inserted in the metal core of the solenoid. The alternating current passes in the solenoid should be increased continuously until the ring begins to elevate. The ring will come to equilibrium at the end of the solenoid. Then by substituting all measured and calculated parameters in equation (2.15), the density of copper can be calculated directly. One might argue the importance of this method as a new method of approach that relates the true characteristic of the material to its density.

2.6.5 Calculations of the magnetization density of the core (M)

The magnetization density of the core is proportional to the external magnetic field B_{ext} (Hammond, 1971). Knowing that B_{ext} depends on the number of dipole moments aligned in the direction of the external field, the maximum magnetization density is reached when all dipole moments are aligned parallel to B. Therefore, the magnetization density is different from one point on the core to another (Portis, 1978). This is because the magnetic field on the core is different and the magnetization density can be written in terms of z coordinate as M (z).

The magnetic field B_z at any point P over the upper edge of the core can be measured with the core (B_{in}), and without the core (i.e., after the removing of the core) B_{ext}. Then by using equation (2.8) we get

$$M = \frac{B_{in} - B_{ext}}{\mu_0} \tag{2.27}$$

2.6.6 Calculations of the core permeability

Since the core consists of ferromagnetic material, both susceptibility χ, and permeability, μ, are not constants. They were both depending on H. The measured B_z at the end of the core was found to fulfill an expression of the form

$$B_{z0} = \frac{\mu IN}{2L} = \frac{emf_{\max}}{nA\omega} \tag{2.28}$$

Solving equation (2.28) for, μ an expression for calculating the magnetic permeability can be written as:

$$\mu = \frac{2L\left(emf_{\max}\right)}{nNIAw} \tag{2.29}$$

2.6.7 Measurements of the magnetic force on the ring

There are several methods to measure the levitation force among, the so called electronic balance method. This method is characterized by several features. Firstly, it is complicated in setting it up. Secondly, there

are some errors that can be introduced when using a balance made of magnetic materials or contains metallic parts.

The general procedure for this method is summarized as follows: by adding non-metallic rings on top of the levitated ring to counter the force on the ring until it returns back to its original place (at the upper end of the solenoid), the weight of all rings will be equal the magnetic force on the ring, this is shown in Figure 2.3.

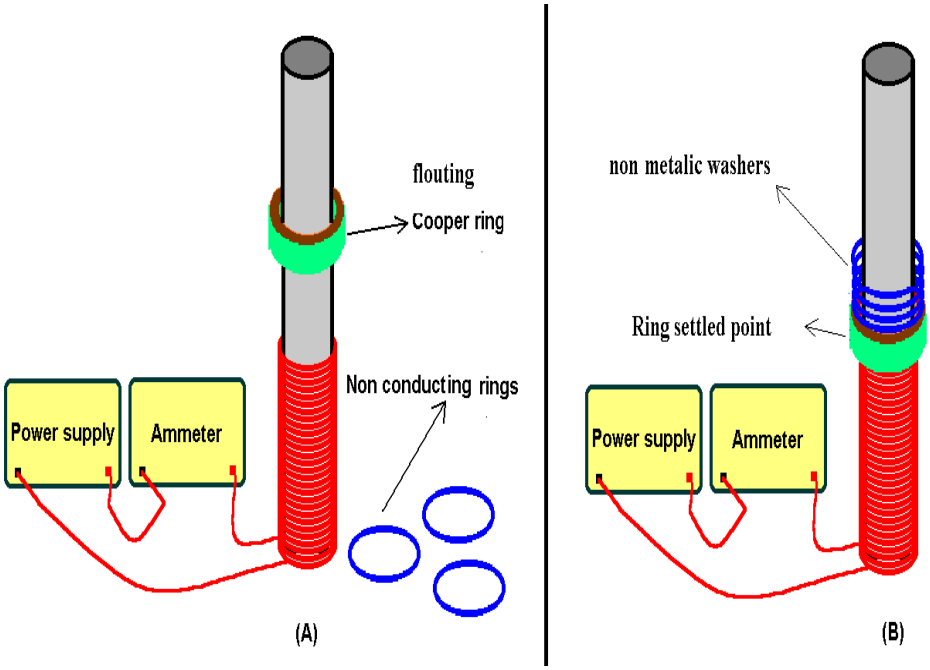

Figure 2.3 Schematic representations showing (a) the solenoid and the non-conducting rings, (b) non-conducting rings added on the top of levitated ring to measure the force on the ring.

Chapter Three

Experimental setup

3.1 Introduction

The eddy current technique is an old one that had been put into use about two centuries ago. In this work, our concentration is on the levitating ring resulting from the induced eddy current in non-magnetic material. Of course, the amount of current produced is dependent on the properties of the material. The experiment and the type of measurements performed are conducted to verify two main objectives in mind. The first one is to investigate the relation between the induced eddy current, as reflected in the form of ring levitation and the properties of ring material. The second objective is looking for new findings concerning the effect itself. As far as the first point is concerned, the study will involve the effect of dependence of the induced eddy current on type of material density, thickness of ring and deliberately introducing defects to the ring such as cracks. The conductivity of the materials, the mean free time between collisions, the specific heat capacity, the number of free electrons per unit volume, the magnetization density, the permeability of some materials and the eddy current induced will be measured and investigated.

The second point deals with measurement leading to more understanding of eddy current mechanism and opens the door for new applications. For example the levitating coil, the high eddy current induced in the ring, the heating substances using electromagnetic waves…etc, can be tested and investigated widely.

A non-magnetic conducting ring inserted in the metal core of a solenoid carrying an AC current is induced magnetic forces which causes the ring to jump up several centimeters had been produced (Restivo, 1996; Avrin, 2000). On one hand, investigating such phenomenon experimentally, the relation between the eddy current induced in the ring and its density, resistance, conductivity…. etc, will be followed. On the other hand, the size of the eddy current and its dependence on ring shape, current in the solenoid and type of material are also of special interest. Accordingly, electrical parameters and properties of material such as brass, aluminum, mercury and silver can be tested and some other properties can be investigated. Thus, several measurements are expected by using diverse experiments. It is worth mentioning that some of experiments are discussed in Chapter 2.

Since eddy currents are induced in conductive materials only, the study will be concerned mainly on investigating ferromagnetic, paramagnetic, and diamagnetic materials. For instance, the study will

include the following materials: copper, aluminum, iron, mercury, silver and gold. In this chapter, the jumping ring experiment is used to investigate the levitation height of aluminum, copper and iron ring samples having different radii and masses. Thus, several rings of these substances are prepared and used throughout this study.

3.2 Measurements and Calculations

Figure 3.1 exhibits the complete experimental apparatus used to collect data. It consists of the following components:

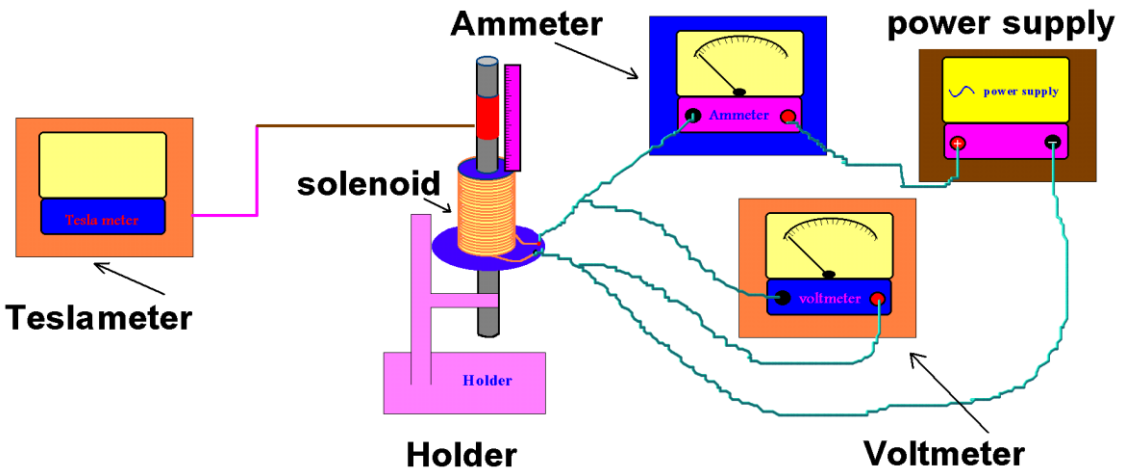

Figure 3.1 Schematic representations showing the jumping ring complete apparatus.

1. Non magnetic rings from different materials (gold, mercury, aluminum, copper, silver), of different thickness and length.

2. Secondary coil

3. Voltmeter

4. Ammeter

5. Teslameter

6. Alternating variable power supply (0-10 A, 0-50 V)

7. Holders

8. Ruler

Before taking measurements, the experimental apparatus has to be tested and calibrated. System testing was conducted out to confirm authentication of the experiments. Apparatus have been assembled on a horizontal table so that the ring is kept vertically. All readings have been measured carefully using sensitive apparatus such as digital multimeter that was used to measure the resistance of the solenoid as well the current and voltage. By making use of Ohm's law, the strength of the magnetic field is calculated as soon as the *emf* induced across a secondary coil is measured (see Chapter 2 section 2.6.1). In addition, the magnetic field strength was calculated theoretically and compared with the experimental results.

As the experimental apparatus was assembled, measurements were started. Each time a certain parameter has to be changed and the measurements are repeated several times. The magnetic field was measured with high percentage (5%) for different current amplitudes up to 3 A. After that, the error percentages were increased as the current exceeds 3 A. All

readings were taken within a shortest possible time in order to make sure that the solenoid is heated to the minimum level. Moreover, the experimental errors in the equipment were estimated as follows:

1- The error in measuring the levitation height is 0.10 cm.
2- The error in the ammeter measurements is 0.001 A.
3- The error in the voltmeter measurements is 0.001 V.
4- The error in the teslameter measurements is 0.10 mT.

In this study, focus is made on measuring many interesting properties of the material, such as: conductivity, permeability, density, magnetization density and the demagnetization factor. Setting standard calibration curves for materials of interest in an industrial world. For example, it furnishes an inexpensive way of making sure of metallurgical process according to the preset properties required.

3.2.1 Measurement of B_r and B_z

3.2.1.1 Measurement of B_z

In this experiment, B_z inside the core needs to be measured and since the probe of the teslameter can not be inserted inside the core, another technique is used. The general trend of this technique is as follows:

Measurements were started by measuring the induced voltage, *emf*, across n turns of a copper wire, winded around the core each having a cross

sectional area, A, and placed in the region of interest where measurement of B_z is required. Then using Faraday's law of induction, B_z can be calculated; while B_r can be measured by setting the turns (horizontally) in the region of interest to measure B_r as displayed in Figure 3.2 (Summner and Thakkrar, 1972). However, the vertical component of the magnetic field, B_z, is equal the direct reading of the voltmeter connected to the coil.

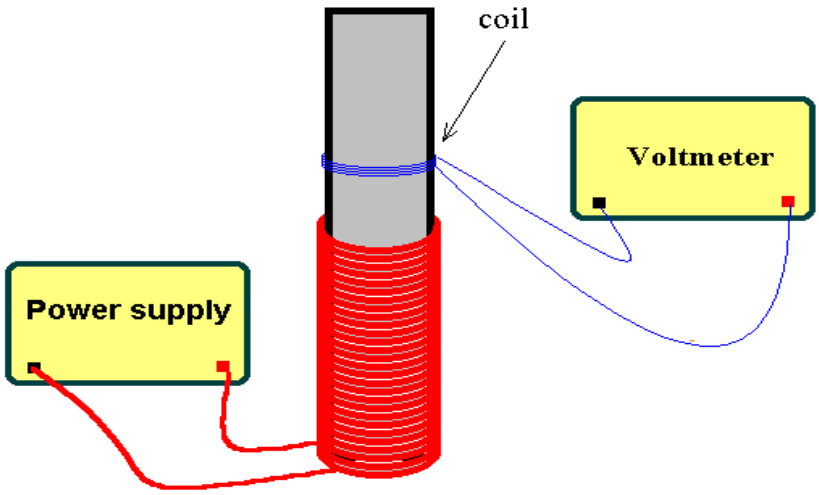

Figure 3.2 Schematic representations showing a coil winded around the metal core through the solenoid used to measure the field in the core.

3.2.1.2 Measurement of B_r

In this experiment, B_r is measured by two ways. In the first one, B_r is measured from point near the core as Figure 3.2 shows. In the second, B_r

is measured from point near the edge of the core when the core brought to level with the solenoid as shown in Figure 3.3.

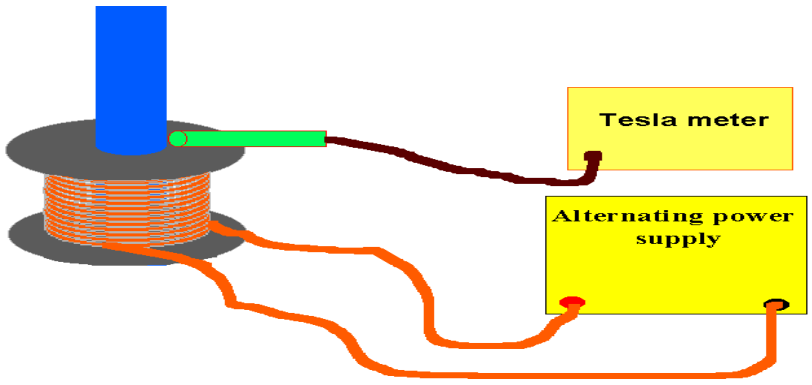

Figure 3.3 Schematic representations showing the apparatus needed to measure the radial component of magnetic field, B_r, from point near the core (1).

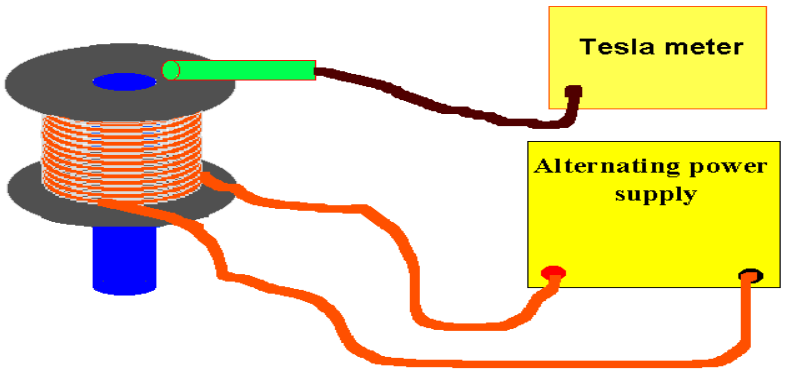

Figure 3.4 Schematic representations showing the apparatus needed to measure the radial component of magnetic field, B_r, from point near the core (2).

3.2.2 Calculation of the conductivity density and number of free electrons per unit volume in copper

In order to measure the conductivity of the ring material using the jumping ring experiment, an annulus ring was inserted in the core passing through a solenoid in which a current can be raised slowly until the ring levitates several centimeters. Once the conductivity is known, the number of free electrons is calculated from the relation between the conductivity (Kip, 1969).

3.2.3 Measurements of the magnetization density permeability of the core and the lowest current needed to rise the temperature of the ring

The magnetization density of the core is proportional to the external magnetic field B_{ext} which depends on the number of dipole moments aligned in the direction of the external field (Hammond, 1971). Thus, at certain fields all dipole moments will be aligned when the magnetization density reaches its maximum value. Therefore, the magnetization density is different from one point on the core to another (Portis, 1978).

The permeability of the core is also a function of z and it can be calculated by measuring B_z at the end of the core.

In measuring the current in the ring connected as shown in Figure 3.5, the current increases until the temperature of the ring began to rise then the current is recorded (Cimate, 2003).

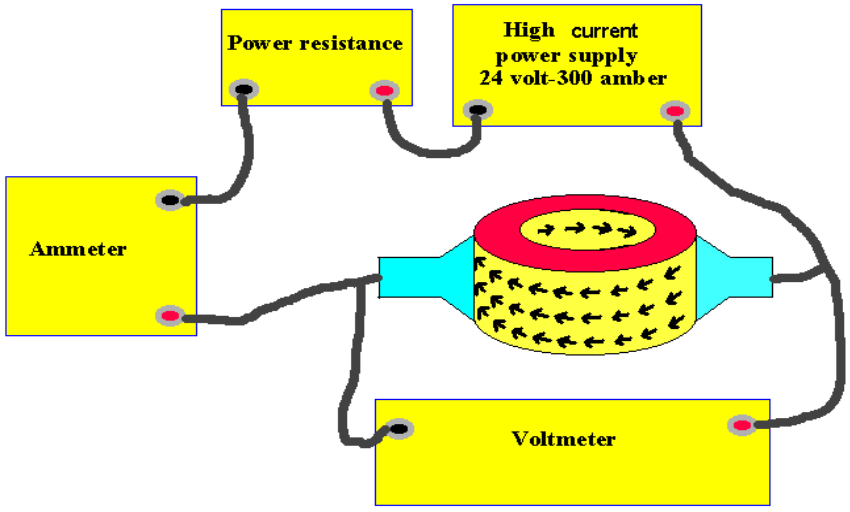

Figure 3.5 Schematic representations showing the apparatus needed to measure the eddy current in the ring.

3.2.4 Measurement of the induced potential across two opposite points on the ring

The induced potential across the ring can be measured by inserting a long ring in the core of the solenoid. A stable alternating voltage across the solenoid coil is applied. The voltage across the ring for different levitation heights can be measured either for the open circuit voltage or the closed circuit voltage by making use of the apparatus shown in Figure 3.6 and Figure 3.7, respectively.

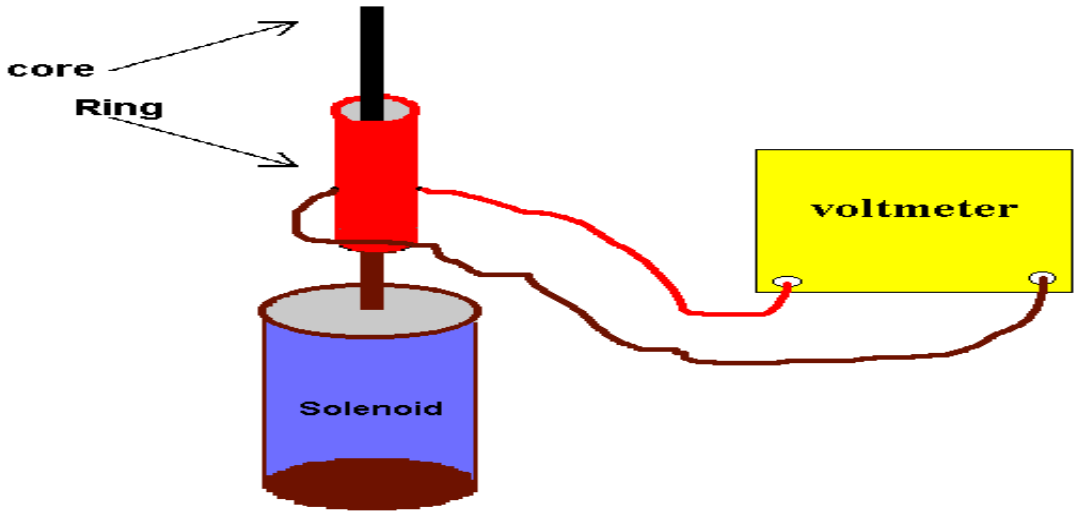

Figure 3.6 Schematic representations showing the apparatus that used to measure the induced *emf* across two opposite points on the ring with longitudinal crack (closed circuit).

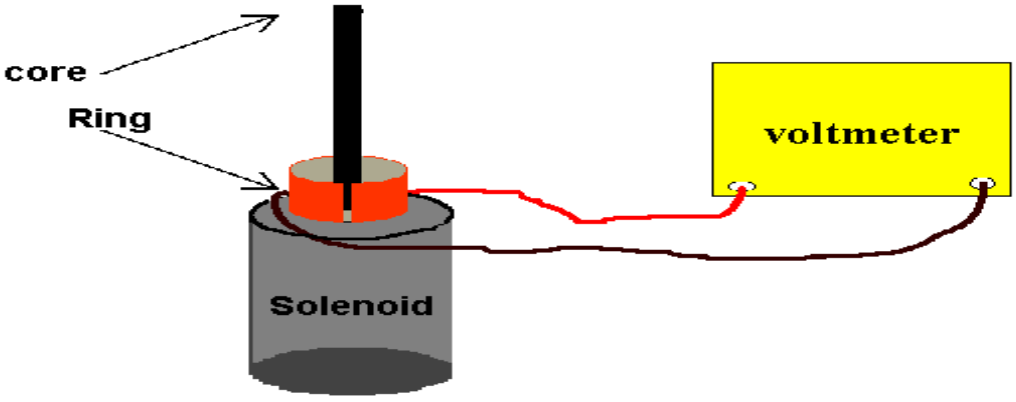

Figure 3.7 Schematic representations showing the apparatus that used to measure the induced *emf* across two opposite points on the ring with longitudinal crack (open circuit).

Chapter Four

Results and discussion

4.1 Introduction

In this chapter, the experimental data are collected using simple experimental facilities described in Chapter 3. Several sets of measurements have been performed for most categories specified in Chapter 3. Each set of data were tabulated and graphically plotted. A brief description of the detection schemes is given. The results reported here are discussed and interpreted theoretically as well. New findings are discovered concerning eddy current technique and many applications were included.

4.2 Results

Results to be discussed here are classified into three categories.

1. The levitation height of ring.
2. Relations between other variables such as the relation between B_r and r, the relation between B_z and z, the relation between either B_r or B and the current passes in the solenoid.
3. Calculations of materials characteristics.

4.3 Results of ring levitation height

4.3.1 Results of magnetic fields

The z-component of the magnetic field, B_z, at the end of the solenoid in terms of the current in the solenoid was measured. The dependence of B_z on the current passing through the solenoid were plotted in Figure 4.1 (see Table A.1 for more details).

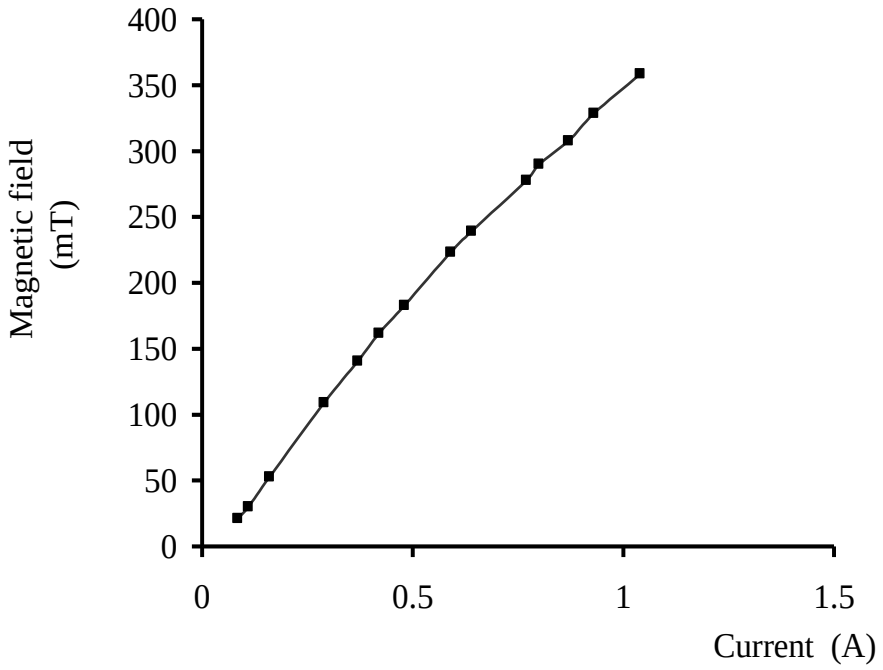

Figure 4.1 Dependence of the vertical magnetic field (B_z) at the end of the solenoid with core on the current in the solenoid

The dependence of B_z on levitation height over the top end of the solenoid are tabulated in Table A.2 and exhibited in Figure 4.2. The general behavior, as the figure displayed revealed that B_z decreases with increasing z. This is in agreement with the theoretical model.

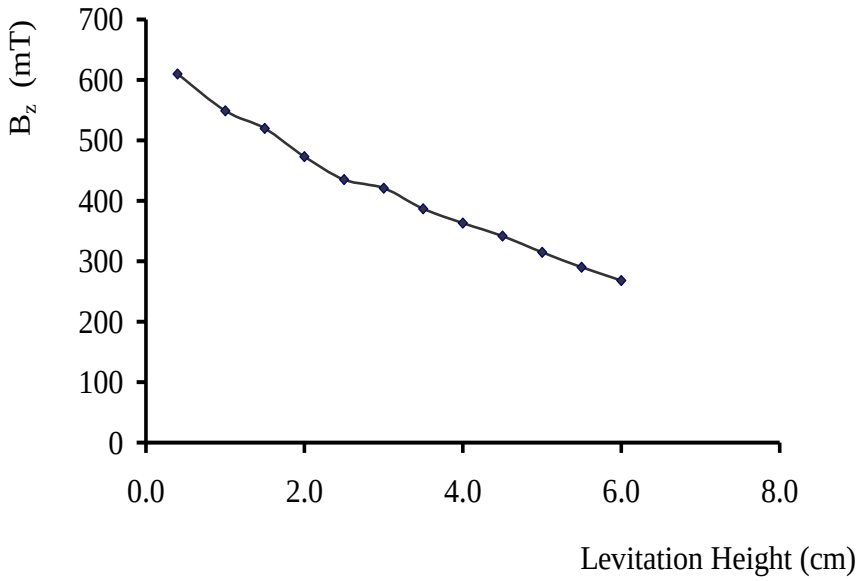

Figure 4.2 Variation of B_z with the height.

Similar measurements were obtained for the radial component of magnetic field, B_r. The results showing the relation between B_r (at the end of the solenoid measured in air above the first turn) and the current in the solenoid are reported in Table A.3 and displayed in Figure 4.3.

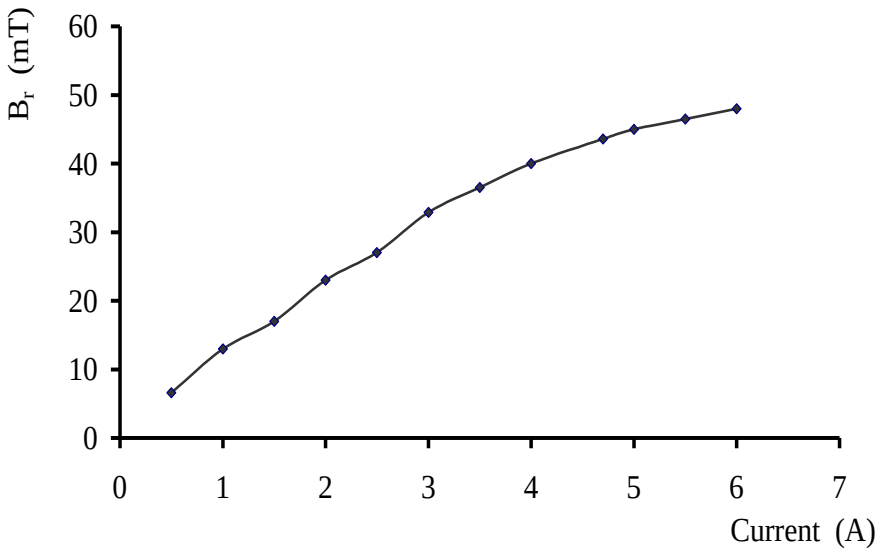

Figure 4.3 Dependence of B_r at the end of the solenoid on the current through it.

According to equation (B.26) and equation (B.35)**,** the magnetic field B is directly proportional to the current I in the solenoid and inversely proportional to z. Therefore, the results exhibited in Figure 4.1, Figure 4.2 and Figure 4.3 are expected.

The dependence of B_r on the radial distance where the core end was brought to level with the top of the solenoid was also investigated. Two interesting cases can be distinguished. The first case is the dependence of B_r on r when the core end brought to the top level of the solenoid. The results were inserted in Table A.4 and displayed in Figure 4.4.

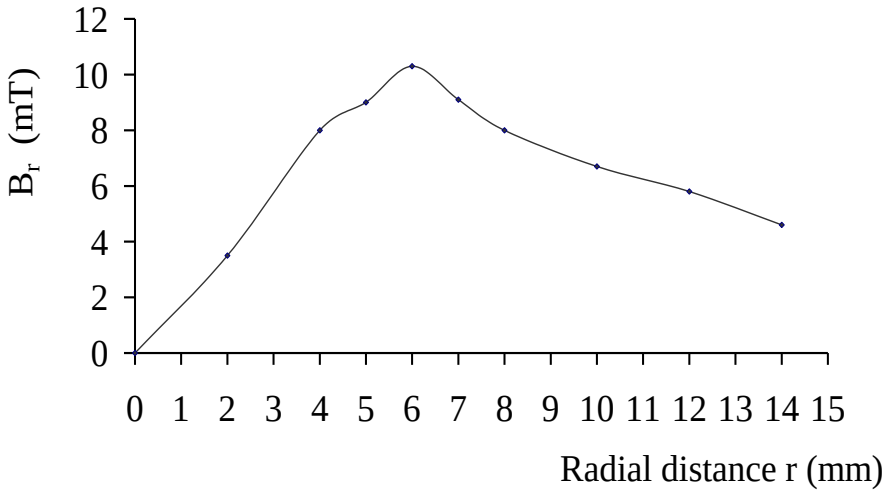

Figure 4.4 Variation of B_r with the radial distance r
rmeasured from center.

As it can be seen from Figure 4.4, B_r exhibits a maximum value at r = 6 mm.

The second case is concerned mainly with investigating B_r dependence on the radial distance measured from the center outward in the direction of increasing r. The results were reported in Table A.5 and plotted in Figure 4.5. Clearly, the highest value of the magnetic field is appeared near the core of the solenoid. This is because the magnetization density near the core is too high. On moving away from the core center in the direction of increasing r, B_r decreases rapidly.

Theoretically, the obtained results can be explained as follows: At the edge center of the solenoid, all field lines are along the z-direction so B_r is

zero. As r increased, B_r increases until r = a then decreases again for r > a. Such variations can be explained as:

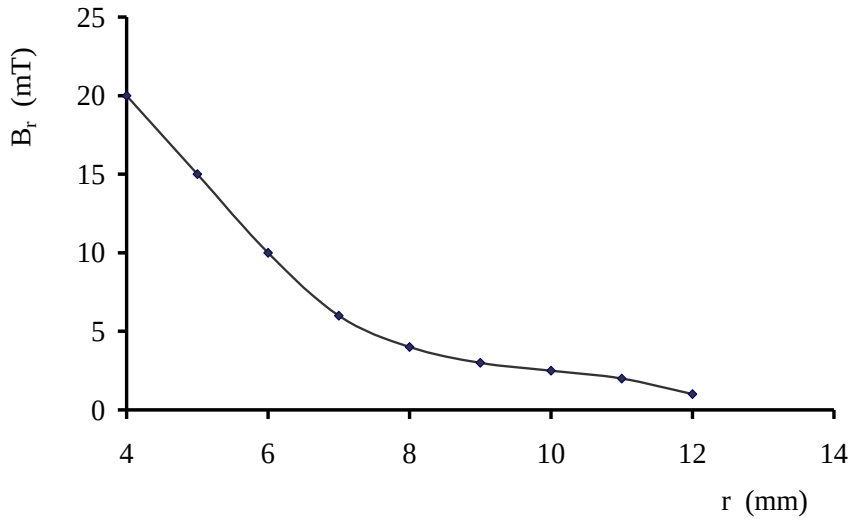

Figure 4.5 Variation of B_r with radial distance (r) measured from point near the core

1. When r < a, and in the direction of increasing r, the distance between the point and the turns of the solenoid decreases until the point become coincidence with rim of the solenoid (i.e. r = a) and hence B increases. After this point the distance increases and B will decrease.
2. The radial component B_r = B cos (θ) (Here θ is the angle between B and r) is zero at the center, where θ = 90° (minimum). As r increases, θ decreases to zero at r = a, and B_r becomes maximum. When r > a, θ

begins to increase again, and B starts to decrease (from its value of part 1). Thus, B_r decreases once again (see Figure 4.6).

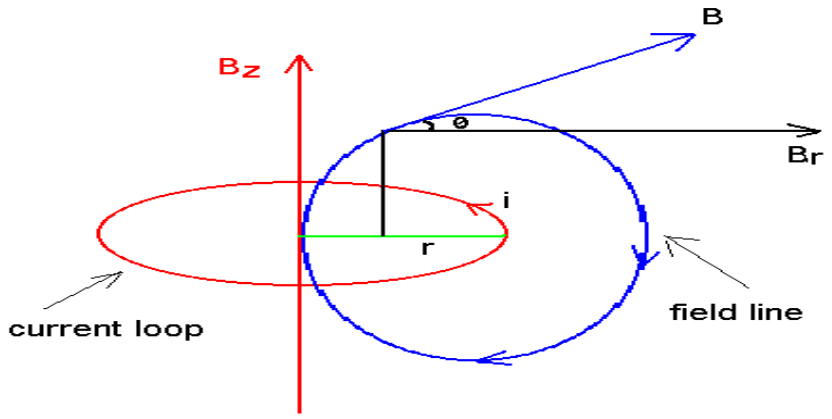

Figure 4.6 Schematic representations showing the field lines of a circular loop and the orientation of B_r.

The experimental results were found to be in good agreement with the theoretical results within 10%.

4.3.2 Results of levitation force

The dependence of the force acting on the ring on the current passing in the solenoid is tabulated in Table A.6 and it plotted in Figure 4.7. The general behavior of the force on the ring placed at the top end of the solenoid was found to be proportional to the square of the current at low current values, but for higher current values it is not. The general behavior of F is shown in Figure 4.8.

Figure 4.7 The dependence of the force acting on the ring on the current passing in the solenoid for low current regions.

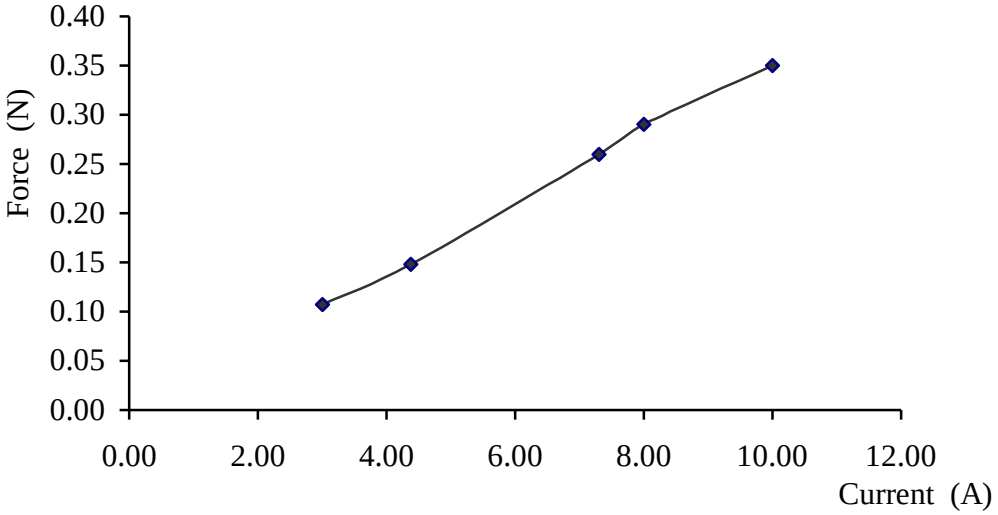

Fig 4.8 The dependence of the force acting on the ring on the current passing in the solenoid for high current regions (3-10) A.

As it could be seen from Figure 4.8 the magnetic force on the ring is not increasing rapidly as the current increase for high current values in the range between 3 and 10 A. This is because most of the electrical energy is converted to heat and this is very well correlated with theory.

4.3.3 Results of ring levitation height

4.3.3.1 Ring levitation height dependence on its length

In this part of the experiment, the relation between levitation height of the ring and its length is investigated. This was simply achieved by preparing rings of different lengths for both copper and aluminum. In each case, every ring was inserted in the core of a finite solenoid and a constant alternating voltage is applied across it. When the voltage is switched on, the ring rises to a certain levitation height. This levitation height is measured as a function of the potential and the current of the solenoid. The magnetic field in the region where the ring jumps is measured near the center of mass of the ring. All measurements should be taken in less than 30 seconds to avoid any increase in temperature of the apparatus (ring, the coil, and the core). Alternatively, a cooling technique has to be employed to control temperature. Results are tabulated in Table A.7 and plotted in Figure 4.9 and Figure 4.10.

Relatively speaking two cases can be identified. On one hand, the levitation height increases as the length is increased (for small rings length). This is because the entire ring will be immersed in a high magnetic field region. On the other hand, the levitation height decreases as the length increases (for long rings length). This is because increasing the ring length above a certain level will produce an increase in the ring mass without

increasing the eddy current induced in it. The extra length falls in the magnetic field at high altitude where field values decreases very rapidly (Portis, 1978).

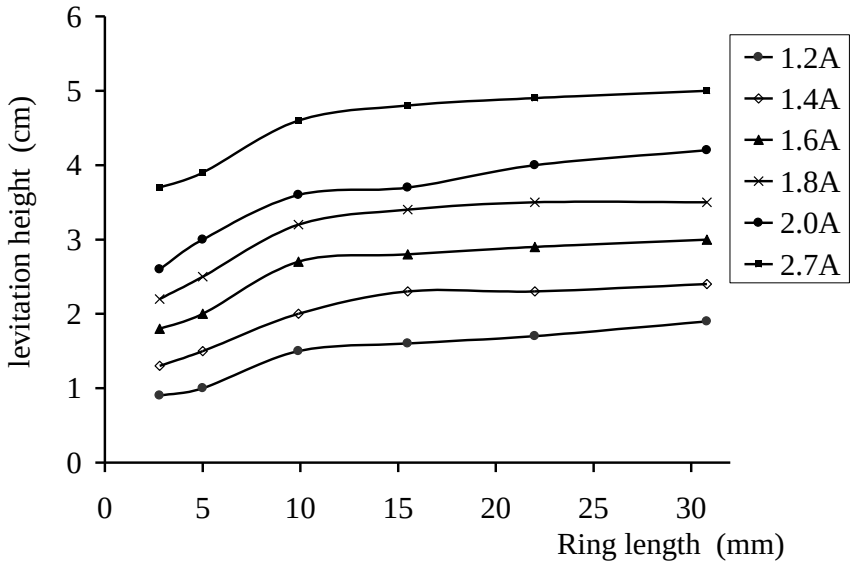

Figure 4.9 Levitation height versus the ring length for different input currents.

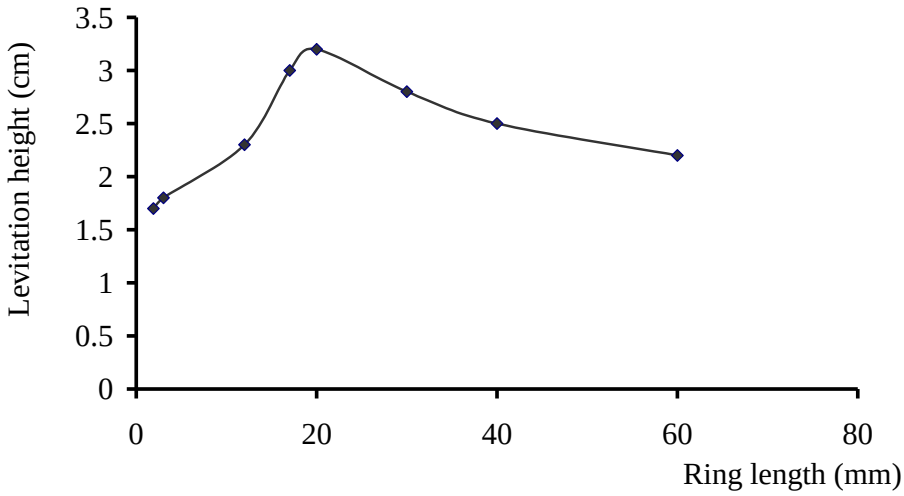

Figure 4.10 Levitation height of the lower end of copper ring versus its length for fixed current.

4.3.3.2 Ring levitation height dependence on its thickness

Investigation of the relation between levitation height of the ring and its thickness is slightly a difficult task due to many considerations. The first one, concerning the manufacture of finding different rings of different thickness from available pipes which is hindered with the problem of internal and external diameters. For example, if a ring is found with the required thickness it might have an internal diameter that is very much larger than the core diameter. This introduces other practical problems as a result of the ring being tilted. Hence different parts of the ring lie in different field regions as shown in Figure 4.11. To overcome the problem, a set of rings were manufactured at different thickness but the entire same diameter (0.4 cm). The corresponding results of this section is shown in Table A.9 and plotted in Figure 4.12.

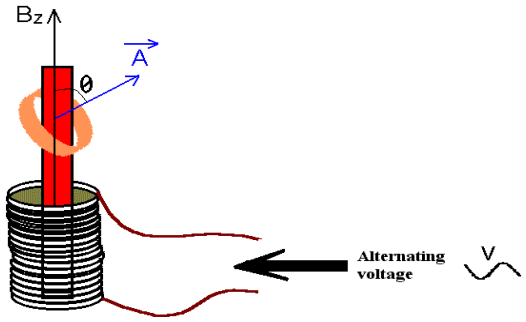

Figure 4.11 Schematic representations showing the effect of gravitational torque on large radius ring.

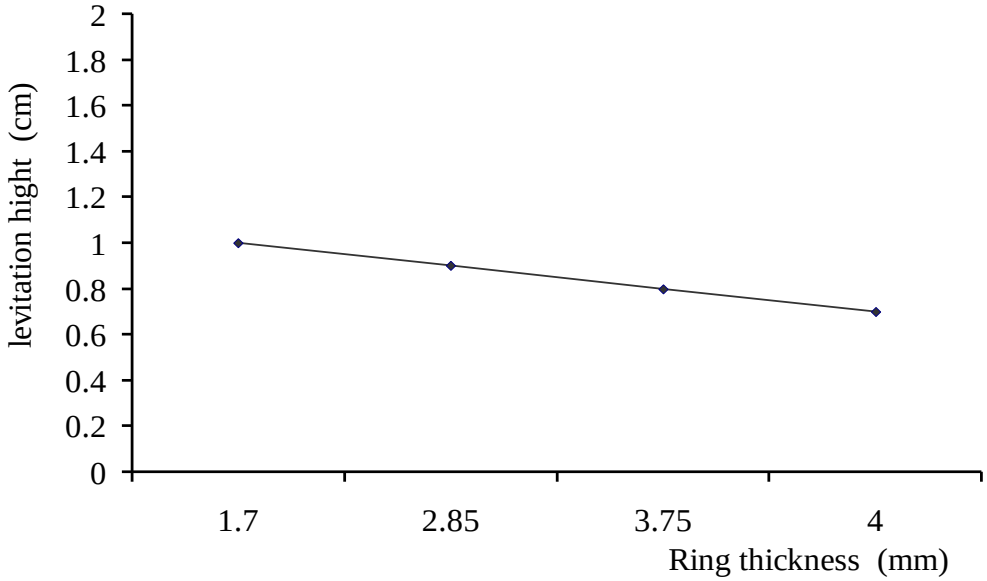

Figure 4.12 The relation between levitation height of different thickness for yellow brass rings, when having a diameter of 4 mm and a fixed input current

4.3.3.3 Ring levitation dependence on thickness and length

Theoretically, when the length or the thickness of the ring increases, its mass also increases. Moreover, when the resistance of the ring decreases, the eddy current is increased. Therefore, the force will be increased if the ring's length and thickness are in the range of the induced magnetic field (Summner and Thakkrar, 1972). The experimental results have shown two cases:

1. For small rings where having lengths vary from 1 to 20 mm, the levitation height increases as the length is increased. This is shown in Figure 4.9.

2. For large rings where length varies from 20 to 70 mm, the length of the levitation height decreases by increasing the length as shown in Figure 4.10.

The results obtained for the jumping ring experiment can be explained simply by imagining the solenoid coil, the ring, and the core as a transformer consisting of two coils. The primary coil (the solenoid coil) and the secondary coil (ring). The only difference between the two cases is that the ring, in this case, is free to move and always make a short circuit.

On the microscopic basis, the results can be explained as follows: When a non-magnetic material is subjected to an alternating magnetic field, an eddy current is generated through it (Restivo, 1996). To understand this result, the rotation of every electron in its orbit will be treated as a dipole moment. In the absence of the external magnetic field, these dipole moments will be distributed randomly as shown in Figure 4.13a. These dipoles are expected to be aligned in a certain way in the presence of external magnetic field (Portis, 1978). It is directed in the opposite direction of the applied external magnetic field according to Lenz's Law as shown in Figure 4.13b.

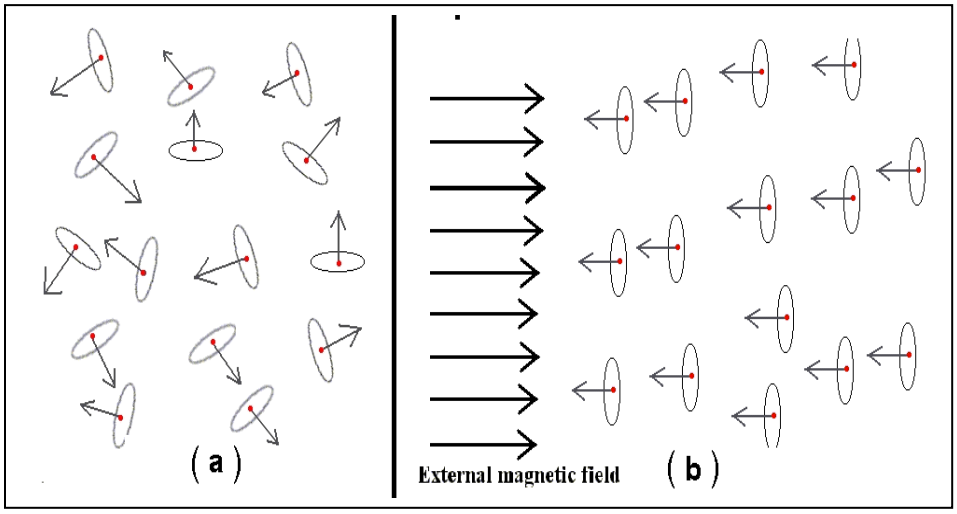

Figure 4.13 Schematic representations of (a) the random direction of the dipole moments in material, (b) the alignment of dipole moments in material when it's placed in an external magnetic field.

Then, a repulsive force will appear between the induced magnetic dipole moments and the dipole moments of the eddy current induced in the ring. Thus, the ring will jump upward and stops at a certain point known an equilibrium point. At this point, the levitation force is equal to the weight of the ring.

On the macroscopic basis, the results can be explained as follows: When alternating current passes in the solenoid, an alternating magnetic field produced in the vacancy of the solenoid. This field has two components, namely the vertical component B_z in the z-direction and the radial component B_r in the radial r-direction (Simpson *et al.*, 2001). The induction of the vertical component B_z through the rings area induced an

emf distributed in the ring. Thus, an eddy current is induced in the ring according to Faraday's law of induction (Halliday *et al.*, 2001). Accordingly, when a section of wire of length *l* carries a current *I* and placed in an external magnetic field B_{ext}, it is experienced a sideways deflection force (Portis, 1978). This force can be calculated according to equation (2.14). Performing the cross product, the radial component as well as the z-component of this force is obtained. It can be easily shown that the action of the radial component of the force, F_r, on the ring is similar to a torque. Therefore, if a ring has a magnetic dipole moment, $\vec{\mu}$ and placed in an external magnetic field, B_{ext}, that makes an angle θ with the dipole moment as shown in Figure 4.11, it experiences a magnetic torque that given by $\vec{\boldsymbol{\tau}} = \vec{\mu} \times \vec{B}_{ext}$. This torque will act to rotate the dipole moments and forces them to align in the same direction of the vertical component of the magnetic field B_z. Hence, the net radial force on the ring is equal to zero as shown in Figure 2.9b. Consequently, the other force component, the vertical force F_z, will cause the ring to jump upward (see Chapter 2 section 2.5). By making use of equation (B.53), it can be easily shown that:

$$F_z \propto B_r B_z \tag{4.1}$$

According to equation (4.1), the levitation force is proportional to both B_z and B_r. This force will cause the ring to levitate upward until an equilibrium point is reached (Hall, 1997). If B_r is zero, the force also will be zero. The dependence of the magnetic force on the ring and the current in the solenoid has two cases:

1. For low current, the magnetic force is proportional to the square of the applied current. This can be seen by substituting the value of B_z and B_r from equation (B.26) and equation (B.35) into equation (B.53).

Thus,

$$F_z = \frac{wtA\sigma\mu^2 N^2 a^2 ri^2}{8L} \int_{z_1}^{z_2} \left[\frac{(z+L)}{f} - \frac{z}{y} \right] \left[\frac{f^3 - y^3}{f^3 y^3} \right] dz = KI^2 \tag{4.2}$$

where

$$K = \frac{wtA\sigma\mu^2 N^2 a^2 r}{8L} \int_{z_1}^{z_2} \left[\frac{(z+L)}{f} - \frac{z}{y} \right] \left[\frac{f^3 - y^3}{f^3 y^3} \right] dz \tag{4.3}$$

Therefore, for low currents, the magnetic force is proportional to the square of the applied current and the experimental results have shown good

agreement with the theoretical (Hall, 1997) (see Figure 4.7).

2. For high currents, the relation between F_z and the current seems to be linear. This means that the magnetic field reaches its saturation value as the relative permeability reaches its maximum value for high currents (Hammond, 1971) (see Figure 4.8).

The force acting on the ring can be interpreted in terms of dipole-dipole interactions. Generally speaking, any two dipole moments μ_1 and μ_2 will attract or repel each other by a force that depends on their orientations and separations. The main cause for such force is the radial magnetic field produced from any one of the rings on another as displayed in Figure 4.14.

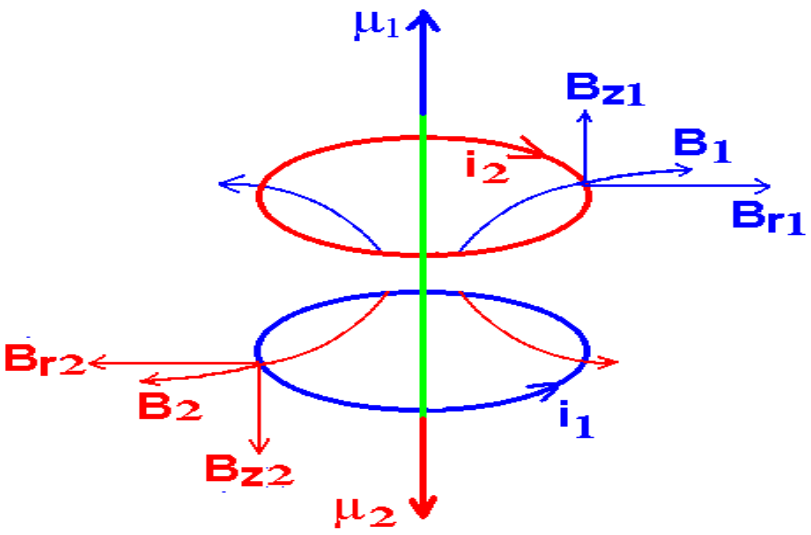

Figure 4.14 Schematic representations showing the interaction between two dipole moments.

As it can be seen from Figure 4.14, the attractive or the repulsive force is attributed to the radial component of the magnetic field B_r produced by one dipole moment on the other. The theoretical relations showing the dependence of B_z and B_r on the current passes in the solenoid coil, which can be obtained from equation (B.26) and equation (B.35). Thus,

$$B_z = \frac{\mu NI}{2L}\left(\frac{(z+L)}{f} - \frac{z}{y}\right) = C_2 I \tag{4.4}$$

and

$$B_r = \frac{Na^2 \mu Ir}{4}\left[\frac{f^3 - y^3}{f^3 y^3}\right] = C_1 I \tag{4.5}$$

Here C_1 and C_2 are constants. Therefore, both of the two components of the magnetic field are proportional to the current developed in the solenoid coil. Thus, when the current passes in the solenoid coil is increased, both B_r and B_z are increased too.

The force was also found to be proportional to B_r B_z. Thus when the applied voltage on the solenoid is increased, the force on the ring will be increased. Consequently, the ring will levitate to higher points. Theoretically, for rings of small lengths, the ring will be placed in the high magnetic field region. Thus, increasing its length means increasing its

weight linearly. Consequently, if the length of the ring, z, or the thickness, t, is increased, its mass will increased linearly accordingly to W= (constant) tz. Also, if the length or the thickness of the ring is increased, its volume is increased. Therefore, the number of free electron will be increased and the current I will be increased as well (I= constant t z). Hence, an increase in both of the induced eddy current in the ring and the levitation force will be expected. This is because the levitation force is proportional to the square of the current i.e. F = constant I^2 = constant $(t\ z)^2$ according to equation (4.1). Therefore, the levitation force is proportional to z^2, but the weight of the ring linearly proportional to both z and t. Thus, the levitation force will be expected to increase by an amount greater than the weight. For an upward F_z and $F_z > W$, the ring will levitate upward.

For long rings, one portion of the ring sinks in the high magnetic field region and the other portion sits in the region were the magnetic field is very low. Hence, an increase in the ring length in this area does not mean an increase in the force on it. As a result, the weight increases while the force still almost constant, so the ring falls down. Furthermore, by using equation (2.14), one may write:

$$\rho = \frac{w\sigma x^2}{2g\mathrm{L}} \int_{z_1}^{z_2} \left(\frac{\mu_0 N I_0}{2L} \left[\frac{(z+L)}{f} - \frac{z}{y} \right] \right) \left(\frac{N a^2 \mu_0 I_0}{4} \left[\frac{f^3 - y^3}{f^3 y^3} \right] \right) dz \qquad (4.6)$$

Rearrange the above equation to get:

$$\frac{16\rho g L \mathrm{L}}{w\sigma x^2 N^2 \mu^2 i_0^2 a^2} = \int_{z_1}^{z_2} \left(\left[\frac{(z+L)}{f} - \frac{z}{y} \right] \left[\frac{f^3 - y^3}{f^3 y^3} \right] \right) dz \qquad (4.7)$$

Introducing $K = \frac{16\rho g L}{w\sigma x^2 N^2 \mu^2 i_o^2 a^2}$ and $F(z) = \left(\left[\frac{(z+L)}{f} - \frac{z}{y} \right] \left[\frac{f^3 - y^3}{f^3 y^3} \right] \right)$.

Then equation (4.6) can be rewritten as:

$$K\mathrm{L} = \int_{z_1}^{z_2} F(z) dz \qquad (4.8)$$

Since the force on the ring is proportional to this integral, equation (4.8) must be integrated in order to find the relation between the length of the ring and its levitation height. For the sake of simplicity, the integral in equation (4.8) is set equal to the area under F(z) and z. Figure 4.15 shows the theoretical relation between F(z) and z.

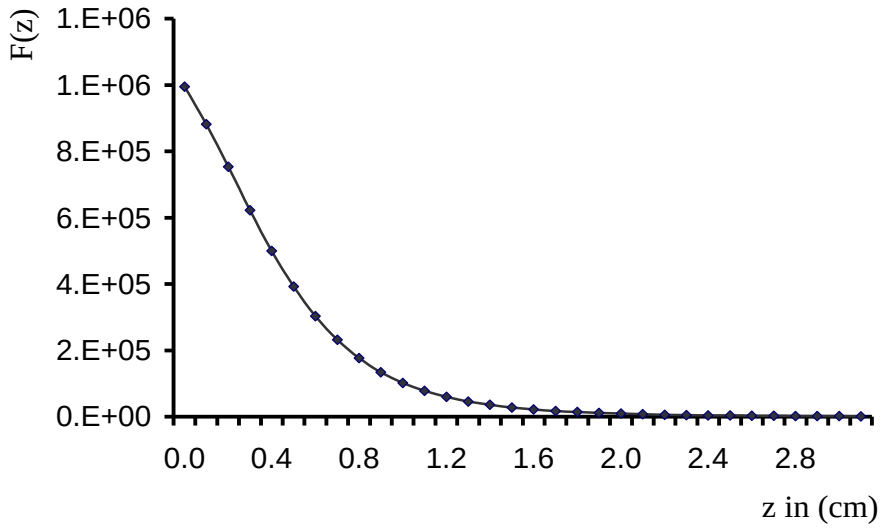

Figure 4.15 Relation between F(z) and z at constant applied current 2 A.

The area under the curve is "nearly" between z = zero and z = 3 cm for constant voltage across the solenoid. The upper limit z = 3 cm depends on the voltage applied to the solenoid, the radius and the number of turns per unit length of the solenoid. The best fit of F(z) between 0 and 3 cm is $F(z) = 10^6 e^{(-226.6Z)}$.

Let the lower end of the ring reach a point on the core z_1, so the magnetic field of the solenoid affect the length of the ring only between z_1 and z_2 (3 cm) and the remaining length have no effect. This part has the effect of increasing the mass of the ring only. In other words, short rings can

reach any levitation height between 0 and 3 cm. Besides, the lower end of any ring must between 0 and 3 cm (see Figure 4.16).

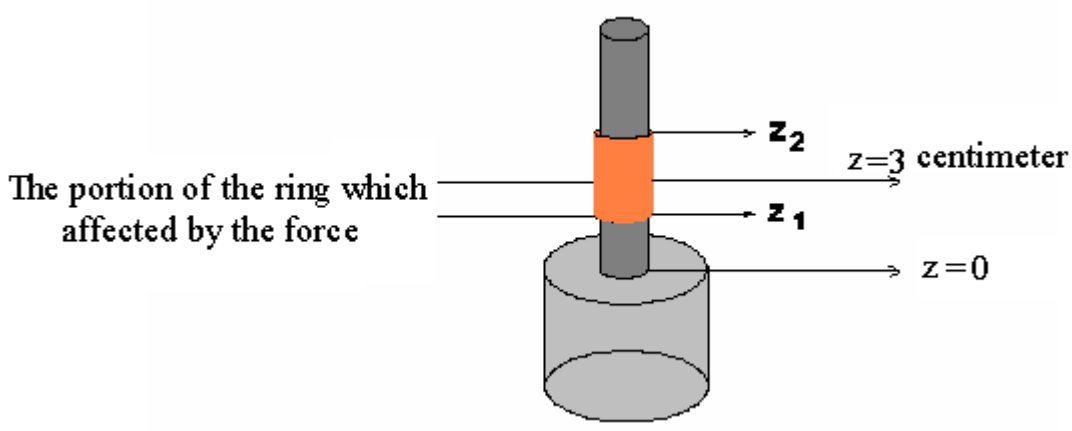

Figure 4.16 Schematic representations showing the portion of the ring affected by the force.

To find the point at which the lower end of the ring z_1 will reach, equation (4.8) must be integrated from z_1 to 0.03 m, after substituting the interpolated expression of F(z) in it (see Figure 4.16). Thus,

$$KL = \int_{z_1}^{0.03} 10^6 e^{(-226.6Z)} dz \qquad (4.9)$$

Introducing the constant c (=226.6), integrating equation (4.9), and solving for z_1 to get

$$z_1 = \frac{\ln\left\{e^{0.03c} - \frac{KL}{10^6 c}\right\}}{c} \tag{4.10}$$

Since the ring is uniform so that its center-of-mass is located at L/2= (z_2-z_1)/2,

$$z_{cm} = \frac{\ln\left\{e^{0.03c} - \frac{KL}{10^6 c}\right\}}{c} + \frac{L}{2} \tag{4.11}$$

Equation (4.11) represents the relation between the levitation height and the length of the ring. This type of dependence is plotted in Figure 4.17.

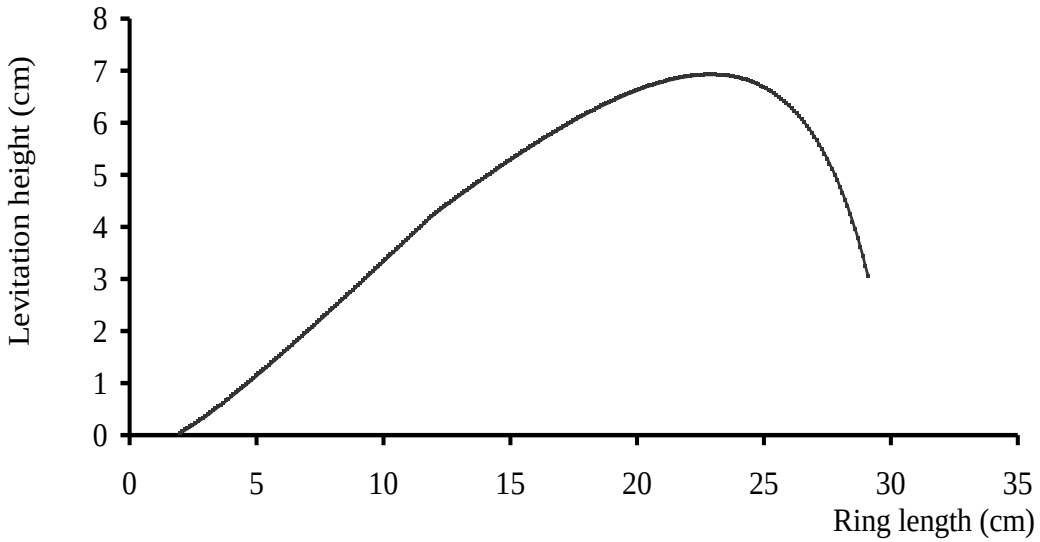

Figure 4.17 Levitation height dependence on length

4.3.4 Induced potential across two opposite points on the ring

The induced potential across the ring was measured by inserting a long ring (10 cm long) in the core of the solenoid. An alternating voltage of 30 V was applied across the solenoid coil. The voltage across the ring for different levitation heights was measured by making use of the apparatus that can be seen in Figure 3.6. No voltage was detected for all rings tried in this lab.

The experimental data has shown that the induced voltage across any two points on the ring is zero. Let R_{int} and R_{ext} to be the internal and the external resistances of the ring, respectively (see Figure B.7). According to Joules law, an amount of energy equal to I^2 (R_{int}+R_{ext}) is dissipated as heat within a time interval dt. During this time, a charge dq = idt will be moved through the emf seat, and the work done on this charge is given by

$$dW = (emf)dq = (emf)Idt \tag{4.12}$$

From the conservation of energy principle, the work done by the *emf* equal the thermal energy in the resistance

$$(emf)Idt = (R_i + R_e)I^2 dt \tag{4.13}$$

Solving for I we obtain

$$I = \frac{emf}{(R_{\text{int}} + R_{ext})} \tag{4.14}$$

Now let us consider a ring cracked longitudinally and having external resistance R_{ext} (see Figure 4.7) connected across it. As R_{ext} goes to zero, the eddy current reaches a maximum value that can be written as:

$$I_{\max} = \frac{emf}{R_{\text{int}}} \tag{4.15}$$

That is, the *emf* is a measure of the open circuit total voltage across any two points such as point c and d shown in Figure B.7. This means that all the electric energy is converted to thermal energy in the internal resistance of the ring. The potential difference between any two points on the ring can be calculated by making use of loop theorem. Thus,

$$V_{AB} = \sum_{i=1}^{n} IR_i - \sum_{i=1}^{n} emf_i \tag{4.16}$$

or

$$V_{AB} = I \sum_{i=1}^{n} R_i - emf \tag{4.17}$$

or

$$V_{AB} = IR_{\text{int}} - emf \tag{4.18}$$

Such that

$$\sum_{i=1}^{n} emf_i = \text{total } emf \text{ across the ring} \tag{4.19}$$

Substitute the value of I from equation (4.15) in equation (4.19) to get

$$V_{AB} = zero \tag{4.20}$$

The above result can be interpreted on the basis of imagining the ring to be divided into many equal parts such that the *emf* produced across each part is emf_i and whose internal resistance R_i. If emf_i is in the opposite direction of I R_i, the summation of these voltages should be equal to zero.

4.3.5 The effect of cracks on the eddy current

In order to investigate the effect of cracks on the eddy current induced in the ring material, various cracks of different length and width were made on rings of the same thickness and length. Some cracks were made vertically, some were horizontally and some were slanted as exhibited in Figure 4.18.

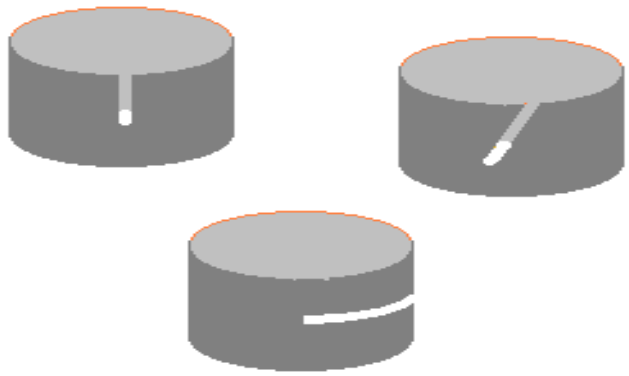

Figure 4.18 Schematic representations showing different cracks that can be introduced to the ring.

The result of some crack characteristics are belonging to an aluminum ring of 26 mm long at various applied currents and the corresponding levitation heights are recorded in Table A.11. The crack length is taken to

be a fraction of the length (L). The dependence of the levitation height on the length and the direction of the crack are shown in Figure 4.19.

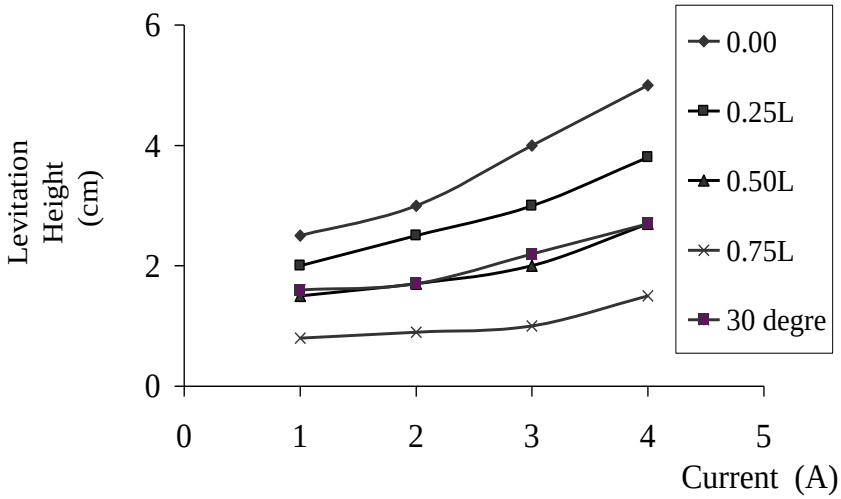

Figure 4.19 Dependence of the length of longitudinal downward crack in the ring, and the corresponding levitation height as current is swept over the range 0.5-4 Amps, one curve to a crack

Relatively speaking, the experimental results had shown a good agreement with the theoretical results. The experimental results can be explained as follows: If the cracks are of longitudinal or makes angle with vertical, the eddy current can not be induced (circulate) in this portion of the ring. Therefore, the resultant eddy current in the ring will decrease and hence the force decreases (i.e. the levitation height decreases). Moreover, if the cracks are latitudinal, the circulation of the eddy current will not be affected. That is, the levitation height will not be affected. Besides, the

current induced in the ring is proportional to the number of free electrons per unit volume (see Figure 4.20).

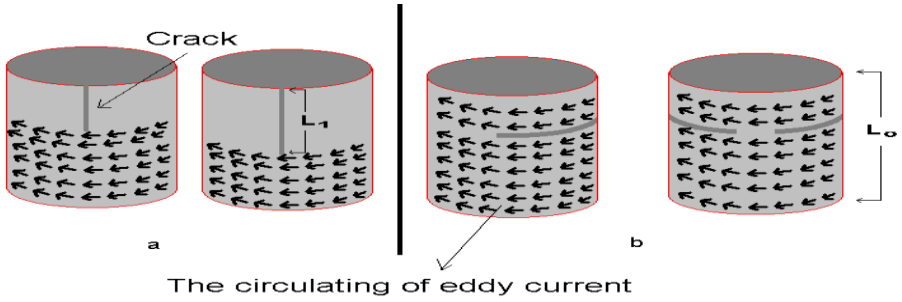

Figure 4.20 Schematic representations showing the circulation of eddy current in the ring with two kinds of cracks
(a) Longitudinal cracks, (b) Latitudinal cracks.

Thus, when the ring is cut vertically the number of electrons allowed to circulate will be decreased by a ratio that depends on the ratio between the non cracked volume and the cracked volume of the ring. So, the eddy current in the cracked ring can be written as:

$$I_c \propto NV_1 \tag{4.21}$$

and

$$I_0 \propto NV \tag{4.22}$$

Thus,

$$\frac{I_c}{I_0} = \frac{NV_1}{NV} = \frac{V_1}{V} = \left(\frac{L_0 - L_1}{L_0} \right) \tag{4.23}$$

Here the symbols are chosen to represent

N is the number of free electrons per unit volume.

I_c is the induced eddy current in the cracked ring.

I_0 is the induced eddy current in the ring without crack.

V_1 is the volume of the non cracked portion of the ring

V_0 is the total volume of the ring.

L_1 is the crack length.

L_0 is the ring length.

4.3.6 Investigations of special non-magnetic rings

In this study, several non-magnetic materials such as gold, silver, aluminum, brass and mercury were investigated. It was found that only the aluminum and bras rings are levitated, while other materials do not. The results of silver, gold and mercury were listed in Table A.12. The rest of the results in tables A.13 to the end belong to aluminum and copper. This might be attributed to low eddy current induced in those materials or the magnetic field is not sufficient to produce such phenomena. Therefore, such problems were still open for further investigations.

4.4 Applications to eddy current measurements

In this section we are interested mainly in investigating some electrical characteristics relevant to the aluminum and copper materials. Five ring samples were used for each material to investigate the dependence of electrical parameters on the material properties such as density, length, mass, thickness, --etc. In the following subsections, calculations of these properties will be discussed.

4.4.1 Calculation of the conductivity

A great amount of heat is usually dissipated in the solenoid or core especially when high currents are used to levitate heavy rings. To avoid this situation, a thin ring of 2 mm long is employed. Some physical parameters, for typical copper and aluminum rings are listed in Table A.13.

The conductivity or density of copper and aluminum can be calculated by measuring the minimum current in the solenoid needed to raise a copper ring of small length a few mm up, using equation (B.64) and the set of parameters listed in Table A.13. The calculated conductivity for copper and aluminum were found to be as follows:

The conductivity of aluminum = $(3.313 \mp 0.0721) \times 10^7$, s/m.

The conductivity of copper = $(5.928 \mp 0.1461) \times 10^7$, s/m

The previously measured conductivities for Al and Cu respectively, are (Kip, 1969):

The conductivity of aluminum = 3.571×10^7 s/m

The conductivity of copper = 5.882×10^7 s/m

The percentage error was estimated to be as 8% or less.

4.4.2 Calculation of the specific heat

The induced eddy current in the ring B resulted in increasing the number of collisions of electron in the ring and hence increases the temperature. The experimental result of the specific heat capacity of aluminum was found to be $0.918 \mp 0.0531, \text{J/g}^0\text{C}$.

Theoretically, the Specific heat can be calculated from the difference between the power delivered in the solenoid before and after the insertion of the ring. This is because such power will be converted to heat in the ring and the solenoid coil (Halliday *et al.*, 2001). The flow of the induced eddy current in the ring causes the temperature to rise as a result of heat dissipation due to collision of revolving electrons in the ring material. The specific heat capacity C of the metal can be calculated by multiplying the measured current in the solenoid before the insertion of the ring I_1 and the current I_2 after the insertion of the ring with the voltage across the solenoid

before and after. If the difference in the current in the solenoid coils (I_2-I_1) is so small, the heat in the solenoid coil can be neglected.

Let ΔQ to be the heat induced in the ring during time τ, the voltage across the solenoid V_{max}, then the amount of heat dissipated is given by (Kip, 1969):

$$\Delta Q = \Delta P \times \tau \tag{4.24}$$

where ΔP the power difference which is defined as:

$$\Delta P = (VI_1 - VI_2) \tag{4.25}$$

If the root-mean-squared (rms) value is used for both current and voltage in equation (4.24) and substituted in equation (4.25), the energy can be rewritten as:

$$\Delta Q = \frac{V_m (I_{m1} - I_{m2})\boldsymbol{\tau}}{2} \tag{4.26}$$

By measuring the initial temperature T_i of the ring, the final temperature T_f, the mass of the ring m, and the elapsed time τ between collisions (see Table A.14), the amount of heat can be also defined as:

$$\Delta Q = C \times (T_f - T_i) \times m \tag{4.27}$$

Equating both of equation (4.26) and equation (4.27) and solving for C, we get

$$C = \frac{V_m(I_{m1} - I_{m2})\,\tau}{2m\,(T_f - T_i)} \tag{4.28}$$

Thus, by measuring the eddy current in the ring and reporting the initial temperature T_i, the final temperature T_f, and the time, the specific heat capacity can be calculated. Introducing E_1 and E_2 parameters as follows:

$$E_1 = V_m \times (I_{m1} - I_{m2}) \times \boldsymbol{\tau} \tag{4.29}$$

and

$$E_2 = 2m \times (T_f - T_i) \tag{2.30}$$

Substituting equation (4.29) and equation (4.30) into equation (4.28), the heat capacity can be rewritten in the following form

$$C = \frac{E_1}{E_2} \tag{4.31}$$

The dependence of E_1 on E_2 For aluminum is plotted in Figure 4.21.

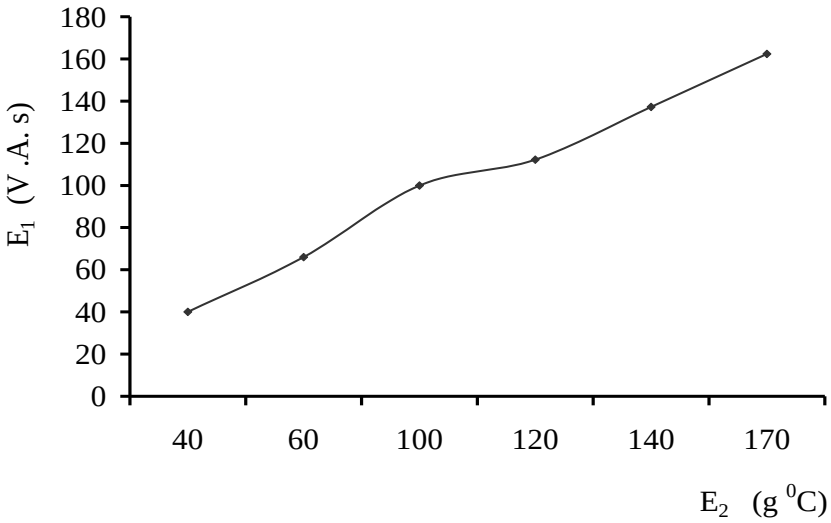

Figure 4.21 Relation between E_1 and E_2 parameteres needed to calculate the specific heat capacity.

The specific heat of aluminum will be calculated from the slope of the curve. The calculated value of C is found to be $0.918 \pm 0.0531 \text{J/g}\,^0\text{C}$. Comparing the obtained value with the corresponding tabulated specific heat capacity is 0.900 J/g ^{0}C (Halliday *et al.*, 2001), the results come to be in agreement within 2%.

4.4.3 Calculations of the number of free electrons per unit volume, and the mean time between electron collisions

The number of free electrons per unit volume can be calculated using equation (2.18) and making use of the estimated value of the mean time between collisions. For example, the calculated mean time between collisions in copper τ is equal to 2.500×10^{-14} s, the electron rest mass m_e = 9.110×10^{-31} kg, the electron charge 1.600×10^{-19} C, and assuming the conductivity is $\sigma = 5.89\times10^{7}$ S/m (Halliday *et al.*, 2001). Substituting all

these variables in equation (2.18), the calculated number of free electron per unit volume, N, for copper is 8.360×10^{28} electron/m^3.

4.4.4 Calculation of magnetization density M and the magnetic field intensity H

As the current passing through the solenoid is increased, both H and M at a certain point on the core is expected to increase. The magnetic field intensity, H, is given by equation (4.33) or $H = \frac{B}{\mu}$. Furthermore, M values can be calculated according to equation (2.21). The calculated values of M, magnetic field intensity, induced voltage and the current in the solenoid are recorded in Table A.16. The dependence of magnetization on magnetic field intensity is displayed in Figure 4.22.

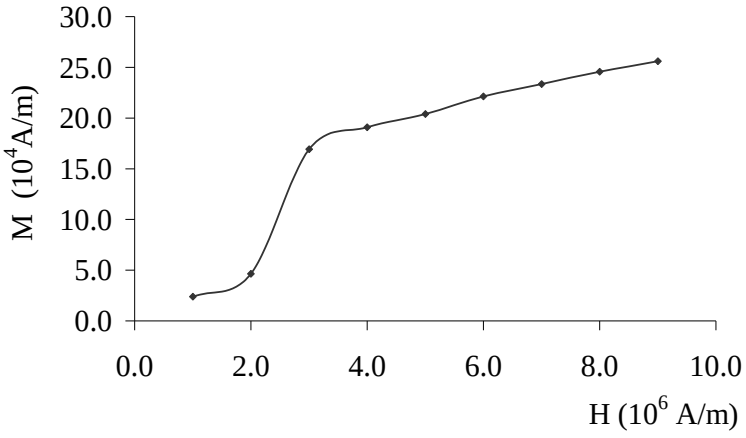

Figure 4.22 Relation betweem the magnetization density M and the magnetic field intensity H for the core metal.

Clearly the magnetization density, M, is not constant, but it depends on the external magnetic field. So by increasing the current in the solenoid, the magnetic field, H, will be increased. Therefore, when external magnetic field is increased, more dipole moments are forced to align in its direction. This means that M increases (since $M = N\mu$), (here N is the number of free electrons, μ is the dipole moment of the electron) until all the dipole moments were aligned. After that, the magnetization density will saturate (Hammond, 1971).

Relatively speaking, the magnetic susceptibility can not be estimated from Figure 4.22. This is because M is not constant. More discussion of magnetic susceptibility is found in section 4.4.6.

4.4.5 Calculation of the relative permeability μ_r

The relative permeability of the material is not constant since it depends on the number of dipole moments which are induced in the material (Hammond, 1971). Moreover, the relative permeability depends on the current through the solenoid in a way such that it increases by increasing the current until it reaches a maximum value. The experimental results showed that the relative permeability of the core is about 144.0 (see Figure 4.23). The maximum value of permeability can be calculated from the curve of B versus H (see Figure 4.22) and using

$$B = \mu H \tag{4.32}$$

Since the magnetization curve for the ferromagnetic material is not linear, the maximum susceptibility is not constant (Kip, 1969). This can be explained as follows: when the current is minimum M increases slowly and as the current increases M increases rapidly to a certain maximum value. In this case, M reaches a saturated value since $\mu = \mu_0(1+\chi)$,where χ is the slope of the magnetization density curve. Thus, for low currents, χ is small and so is μ. As the current is increased, χ is increased too and so is μ. For high currents, both χ and μ become constants. The maximum value for the relative permeability is obtained from the plot of the relative permeability and the current in the solenoid as shown in Figure 4.23. The obtained results of relative permeability can be used to calculate the core permeability using (Portis, 1978):

$$\mu = \mu_0 \mu_r \tag{4.33}$$

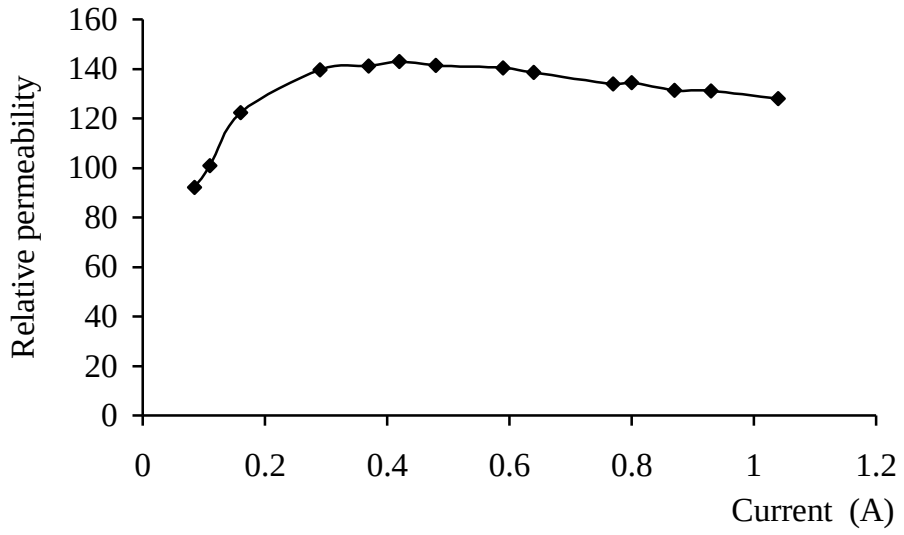

Figure 4.23 Relation between the relative permeability of the core versus the current in the solenoid.

4.4.6 Calculation of the magnetic susceptibility χ

The obtained values of the relative permeability $\mu_r (=144.0)$ and the permeability of air μ_o were used to calculate the value of χ according

$$\mu = \mu_0(1+\chi)$$

$$\chi = \frac{\mu - \mu_0}{\mu_0} = (\frac{\mu}{\mu_0} - 1) \qquad (4.34)$$

The calculated value of χ 143.0.

4.4.7 Calculation of the eddy current induced in the ring

In order to measure the induced eddy current in the ring using conventional methods, the ring must be cut vertically and it should be connected in series with an ammeter. This method is not practical in this

study, due to large internal resistance of the ammeter with respect to the resistance of the ring. Therefore, attention should be directed on finding new techniques to measure such currents. Several techniques for calculating the induced current in the rings are suggested. The First method is the energy method which is based mainly on the energy delivered in the ring and the power delivered by the current. The second method is based on measuring the induced voltage across the ring and making use of Ohm's law. The third method is a comparison between different currents. We shall discuss the above methods briefly.

4.4.7.1 Calculation of the eddy current using the heat dissipation method

By measuring the difference in the power delivered in the solenoid before and after the insertion of the ring, the eddy current can be calculated. Thus, this method depends mainly on the heat dissipated in the ring in the form of heat as a result of flowing eddy currents through. It is found that when the ring is inserted in the core, the current passing through the solenoid is increased. This is because the generating current is not constant. Experimental data shows that an eddy current of 183 A is obtained. This means that the difference between the powers consumed by the solenoid before and after the insertion of the ring is equal to the power dissipated in

the ring. If the initial power delivered to the solenoid without the ring is P_1, the final power with the ring is P_2, and the power in the ring is P, the power dissipated in the ring can be written as:

$$P_2 - P_1 = P \tag{4.35}$$

Using $P = IV = I^2R$, equation (4.35) can be rewritten as:

$$I^2R = V(I_2 - I_1) \tag{4.36}$$

Here I_1 and I_2 are the currents passing through the solenoid before and after insertion of the ring, V is the voltage applied to the solenoid, R is the ring resistance, and I_{eddy} is the eddy current in the ring. Using $R = \frac{l}{\sigma TL}$, the eddy current I_{eddy} can be calculated according

$$I_{eddy} = \sqrt{\frac{\sigma TLV(I_2 - I_1)}{l}} \tag{4.37}$$

Using the experimental values listed in Table A.14 for the variables in equation (4.37), the calculated eddy current value passing in (copper ring) is found to be 183 A. To our knowledge no reference is made to the value of eddy current before.

4.4.7.2 Calculation of the eddy current by measuring the *emf*

In this method, the *emf* between two opposite points on the open circuit ring (see Figure 3.7) was measured for different materials using Ohm's law and the data which presented in Table A.17. The equation used to calculate the eddy current is obtained by making use of $emf = I_{eddy} R$ and $R = \frac{\sigma l}{2TL}$. Thus, the obtained eddy current relation can be written as:

$$I_{eddy} = \frac{emf}{R} = \frac{emf\,(2TL)}{\sigma l} = \frac{emfTL}{\pi \sigma r} \tag{4.38}$$

Where $l = 2\pi r$, and T, r, L, are defined before. The resistance between two opposite points on the ring is R. The calculated value of the eddy current in aluminum ring also is 181 A.

It is worth mentioning here that for aluminum and iron, the induced voltage is the same as copper, but the measured current is different since the conductivity is different.

4.4.7.3 Dependence of ring temperature on time

The electric energy drawn by the solenoid is converted to magnetic energy and heat in the coil core and in the ring. Therefore, the temperature of the ring will be increased as the number of electron collisions in the ring

is increased. It is found that the temperature of the ring is increased with time until it reaches an equilibrium point. Consequently, the coil resistance is increased; while the induced current is decreased. Besides, the magnetic force on the ring is decreased and the levitation height of the ring is decreased with time. The relation between the temperature of the ring and time are presented in Table A.14 and displayed in Figure 4.24.

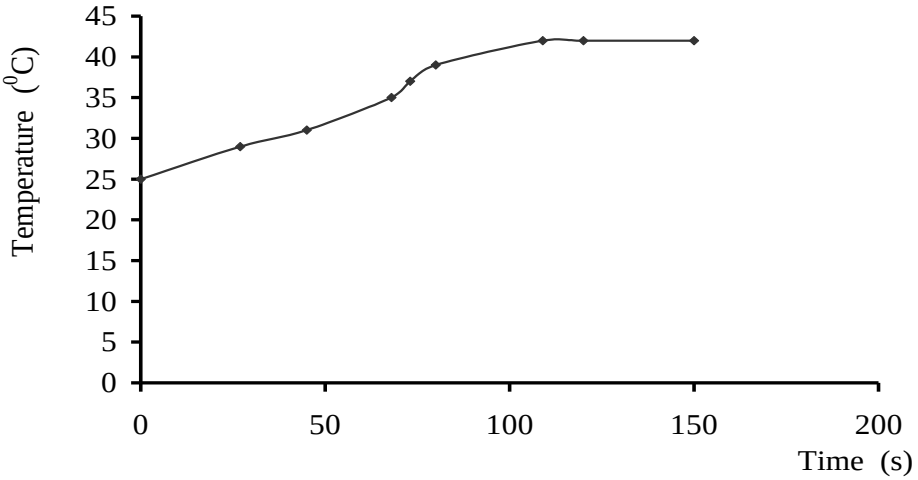

Figure 4.24 Relation between the temperature of copper ring versus time.

4.5 The effect of ring dimension on the current drawn by the solenoid

The current drawn by the solenoid was measured for a solenoid with different rings of various thicknesses and length. Results are tabulated in Table A.18 and Table A.19 and plotted in Figure 4.25 and Figure 4.26.

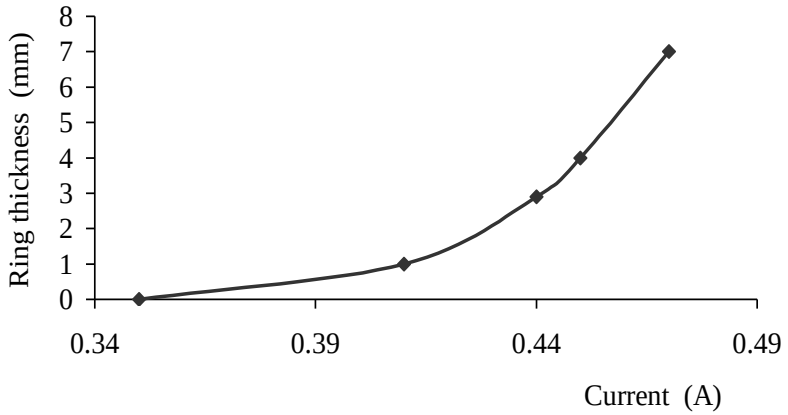

Figure 4.25 The relation between the current in the solenoid coil and the thickness of Aluminum ring for fixed rings length .

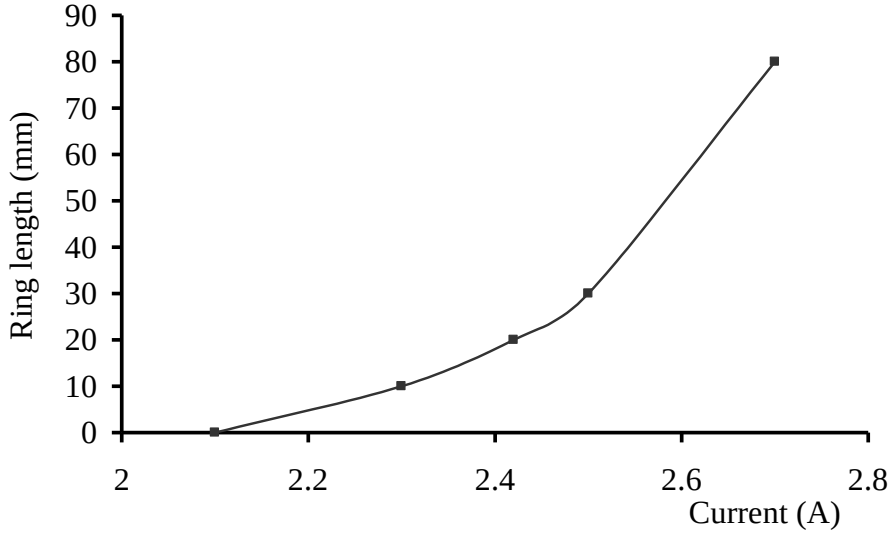

Figure 4.26 The relation between the current in the solenoid coil and the length of copper ring for fixed rings thickness.

In discussing these results, we would say that the solenoid and the core can be imagined as electric device which looks like a transformer. In this case, as the load resistance of the secondary coil decreases its current increases. In other words, the primary current is increased in the ring when either the length or the thickness of the ring is increased. Therefore, its resistance will be decreased. This means the number of free charges per unit volume is increased. Thus, the eddy current in it increases and consequently the current drawn by the solenoid also increases since the energy is conservative (Halliday *et al.*, 2001).

4.6 The levitating solenoid

Consider a solenoid that moves freely about the core. If an alternating current passes through the solenoid, it levitates several centimeters depending on the current and the number of turns of the solenoid. This finding was not mentioned or discussed up to our knowledge so far anywhere else**.**

The force between the solenoid coil and the core is an attractive force and is directed toward a region of high magnetic field (toward the center of the coil). The maximum magnetic field at the center of the coil extends several centimeters near the two ends of the solenoid. This depends on the applied current in the solenoid. Therefore, the solenoid will move upward

until all the extended region filled with the core. Thus, when the current passing through the solenoid is increased, the solenoid jumps more higher (see Figure 4.27).

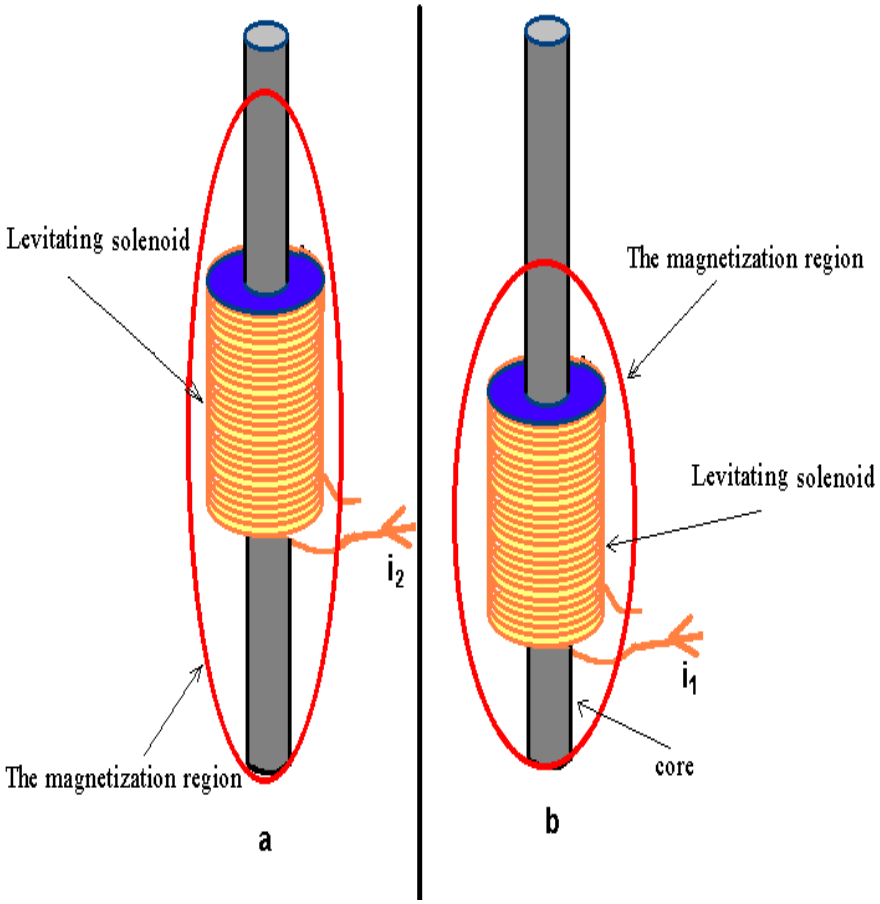

Figure 4.27 Schematic representations showing the extended magnetization area inside the ellipsoids for two currents i_1 and i_2 such that $i_2 > i_1$.

It is noticed that this effect is not observed before; no references had been mentioned referred to it, since coils are mostly manufactured either fixed to the base or to the core.

Chapter Five

Conclusion and further work

If a non-magnetic material is subjected to an alternating external magnetic field, an eddy current is induced in it. In general, the eddy current technique has many applications in applied sciences and especially in physics. The use of eddy current technique in this context is to study some characteristics of non-magnetic materials such as conductivity, mobility, permeability, magnetization of substances, and the numbers of free charges are of great importance. These properties can be studied by knowing the strength of the eddy current produced in a jumping ring made from the material of interest. The strength of the eddy current induced in the material depends on its physical properties, (density, conductivity, volume, temperature,) magnetic properties (paramagnetic, diamagnetic, or ferromagnetic) and also on the external applied magnetic field.

The eddy current induced in materials was studied using the jumping ring experiment. It was found that different substances are not equally affected when experimental conditions were set fixed. The experimental results were found to be in agreement within 8% with the theoretical ones. For conducting materials, the magnetic force on the ring is proportional to

both the vertical and the horizontal components of the magnetic field. Besides, the conductivity was calculated from the equilibrium point reached by the ring above the upper end of the solenoid. This point is independent of the thickness or the length of the ring. Also the potential difference produced across the ring is zero. At the center of the coil there are two radial fields equal in magnitude and opposite in directions. One of the fields is produced by the upper half of the coil turns and the other from the lower half of the coil turns. Therefore, the net horizontal component of the magnetic field B_r at the center of the solenoid coil should be equal to zero. Moreover, since the levitation force is proportional to B_r, the ring can not be stable at the center of the solenoid. If two rings are inserted in the core, an attractive force appears between them since the eddy current induced in the two rings is in the same direction. Accordingly, both opposing fields repel each others. Furthermore, the force between any two successive turns of the solenoid is attractive to each other because the current in one is in the same direction. The drawn current by the solenoid coil increases if either the thickness or the length of the ring is increased. This is due to the increase of power in the ring. Thus, the power in the solenoid has to increase according to the principle of conservation of energy (Halliday *et al.*, 2001). As the current in the solenoid is increased, the levitation height of the ring is

increased. It was found experimentally that the levitation height depends on the type of the material. Among all materials used, only copper and aluminum rings levitate. It was found that the ring began to loose levitation height as time passes. This is due to the increase in temperature and this in turn resulted in decreasing the material conductivity. Hence the eddy current is decreased as well.

Since the levitation height of the ring depends on its electric and magnetic properties. This allows a test that can be used to distinguish between samples purity of the same material.

In conclusion, the jumping ring technique is an important application of the eddy current and a good example of Lenz's law. In this case, the magnetic field is changing due to the AC voltage applied to the coil and the ring placed in the core passing through the solenoid is caused to levitate. This is due to eddy currents created by the changing magnetic field from the coil. The polarity of the eddy current fields will be in opposite (creating a north pole at the bottom of the ring when there is a north pole at the top of the coil, and vice versa) to the coil polarity. Thus, a constant repulsion between the two fields will be observed and the ring levitation height is maintained.

It is also worth to mention that a jumping coil was noticed for the first time. The above effect constitutes a good technique for testing material properties in a simple, inexpensive and an easy experimental system to run.

The study tested samples of other materials such as gold, silver and mercury where no levitation height has been observed even though they are none-magnetic materials. The reason behind this can not be explained on the basis of apparatus used. Thus, such phenomenon is not well understood to us. It is suggested that this is left as an open problem to be addressed for further investigations. Maybe different system needs to be designed that can handle very much higher currents in the solenoid, hence creating higher eddy current in these materials. If levitation height was not noticed, then other reasons must be investigated and our thinking is directed to the internal microscopic structure of these materials.

Appendix A

Tables of experimental data

Table A.1 Data of the magnetic field B_z at the end of the solenoid and the current in the solenoid

Current in the solenoid ±0.001, A	**Magnetic field B_z (mT)±0.100**
0.085	21.00
0.110	30.00
0.160	53.00
0.290	109.0
0.370	141.0
0.420	162.0
0.480	183.0
0.590	223.0
0.640	239.0
0.770	278.0
0.800	290.0
0.870	308.0
0.930	329.0
1.040	359.0

Table A.2 Data of the magnetic field B_z of the solenoid with core versus levitation height (z) over the top of the solenoid at constant current of (3 A).

Levitation height of measurement ±0.100, (cm)	**Magnetic field B_z ±0.100, (mT)**
0.400	610.0
1.000	549.0
1.500	520.0
2.000	473.0
2.500	435.0
3.000	421.0
3.500	387.0
4.000	363.0
4.500	342.0
5.000	315.0
5.500	290.0
6.000	268.0

Table A.3 Data of the magnetic field (B_r) at the end of the solenoid directly above the first turn and the current passing through the solenoid.

Current in the solenoid±0.001, (A)	**Magnetic field ±0.100, (mT)**
0.500	6.600
1.000	13.00
1.500	17.00
2.000	23.00
2.500	27.00
3.000	32.90
3.500	36.50
4.000	40.00
4.700	43.60
5.000	45.00
5.500	46.50
6.000	48.00

Table A.4 Data of the magnetic field B_r at the end of the solenoid and the radial distance r at constant input solenoid current of 1 A

.

Radial distance, r,±0.010, (mm)	**Magnetic field in±0.100, (mT)**
0.000	0.000
2.000	3.500
4.000	8.000
5.000	9.000
6.000	10.30
7.000	9.100
8.000	8.000
10.00	6.700
12.00	5.800
14.00	4.600

Table A.5 Data of B_r and the radial distance from the core (r) measured at the top of the solenoid for constant solenoid current of 2 A.

r ± 0.010, (mm)	**B_r ± 0.100, (mT)**
4.000	20.00
5.000	15.00
6.000	10.00
7.000	6.000
8.000	4.000
9.000	3.000
10.00	2.500
11.00	2.000
12.00	1.000

Table A.6 The induced *emf*, the current, the magnetic field, belong to a copper ring rests at the end of the solenoid for 20 mm ring length.

Lowest mass ±0.010, (gm)	**Induced voltage in the secondary coil ±1.000, (mV)**	**Current in the solenoid ±0.001 ,(A)**	**B_z ±0.100, (mT)**	**B_r ±0.100, (mT)**
4.700	24.00	2.000	348.0	2.400
5.300	26.00	2.200	377.0	2.500
6.800	29.00	2.500	421.0	3.000
8.200	32.00	2.700	464.0	3.500
10.70	36.20	3.000	525.0	4.700
14.80	43.00	4.380	624.0	5.000
26.00	51.20	7.300	743.0	5.500
29.00	57.00	8.000	800.0	6.100
35.00	62.30	10.00	830.0	7.200

Table A.7a The dependence of the center of mass levitation height on the length of copper ring at different applied currents.

Ring length ± 0.010, (mm)	30	20	17	12	13	1.9
Current ± 0.001, (A)	**Levitation height of the center of mass of the ring in ± 0.100, (cm) from solenoid top**					
1.700	NL*	NL	NL	NL	NL	0.200
2.200	3.200	3.100	3.100	2.600	2.000	1.700
2.400	3.300	3.200	3.200	2.800	2.200	2.000
2.600	3.600	3.400	3.400	3.100	2.400	2.200
2.800	3.800	3.600	3.600	3.400	2.600	2.400
3.000	4.000	3.900	3.800	3.600	2.800	2.500
3.200	4.200	4.100	3.900	3.800	3.000	2.600
3.400	4.400	4.200	4.100	4.500	3.100	2.800
3.600	4.500	4.300	4.200	4.100	3.200	3.000
3.800	4.600	4.500	4.300	4.200	3.300	3.100
4.000	4.800	4.600	4.500	4.300	3.400	3.200

NL*: No levitation height of center of mass was recorded

Table A.7b The dependence of levitation height of a copper ring on length (for a long ring) at an applied current of 2.2 A.

Rings length ± 0.010, (mm)	**Levitation height ± 0.100, (cm)**
1.900	1.700
3.000	1.800
12.00	2.300
17.00	3.000
20.00	3.200
30.00	2.800
40.00	2.500
60.00	2.200

Table A.8 Thickness, length, and outer diameter of various rings of yellow copper.

Ring thickness ± 0.010, (mm)	**t1**	**t2**	**t2**	**t4**
	1.700	2.850	3.750	4.000
outer ring diameter ± 0.010, (mm)	11.00	13.30	15.50	17.00
The length of the ring ± 0.010, (mm)	5.000	5.000	5.000	5.000

Table A.9 The levitation height, the thickness of yellow copper rings for two different currents in the solenoid at fixed interior radius (r_1).

The current in the solenoid = 7.240 ± 0.100A		**The current in the solenoid = 4.000 A**	
Levitation height ± 0.100, (cm)	**Thickness ± 0.010, (mm)**	**Levitation height ± 0.100, (cm)**	**Thickness ± 0.010, (cm)**
1.900	1.700	1.000	1.700
1.800	2.850	0.900	2.850
1.600	3.750	0.800	3.750
1.400	4.000	0.700	4.000

Table A.10 The induced *emf* across copper and aluminum rings having 0.77 mm thickness and 11 cm long for different heights along the ring, when the potential across the solenoid coil 30 V.

Levitation height over the top of the solenoid ±0.100, (cm)	**The induced potential across Al ring ±1.000, (mV)**	**The induced *emf* across Cu ring ±1,000, (mV)**
0.000	0.000	0.000
2.000	0.000	0.000
4.000	0.000	0.000
6.000	0.000	0.000
8.000	0.000	0.000
10.000	0.000	0.000

Table A.11 Crack properties, the current in the solenoid and the corresponding levitation heights for aluminum ring of 26 mm long.

Crack direction	**Crack length**	**current in the solenoid ± 0.001 ,(A)**	**Levitation height of the ring ± 0.100,(cm)**
Longitudinal	0.000	2.380	2.500
Longitudinal	0.000	3.000	3.000
Longitudinal	0.000	3.380	4.000
Longitudinal	0.000	4.260	5.000
Longitudinal	0.250 L	2.380	2.200
Longitudinal	0.250L	3.000	2.800
Longitudinal	0.250L	3.380	3.800
Longitudinal	0.250 L	4.260	4.800
Longitudinal	0.500 L	2.380	2.100
Longitudinal	0.500 L	3.000	2.700
Longitudinal	0.500 L	3.380	3.600
Longitudinal	0.500 L	4.260	4.500
Longitudinal	0.750 L	2.380	2.000
Longitudinal	0.750L	3.000	2.500
Longitudinal	0.750L	3.380	3.400
Longitudinal	0.750L	4.260	3.800
30 Degree with vertical	0.500 L	2.380	2.200
30 Degree with vertical	0.500 L	3.000	2.700
30 Degree with vertical	0.500 L	3.380	3.700
30 Degree with vertical	0.500 L	4.260	4.500

Table A.12 Parameters of gold, silver and mercury were used in levitation ring experiment.

Type of substance	The potential across the solenoid coil ±0.001,(volt)	The length of the ring ±0.010,(mm)	The thickness of the ring±0.010, (mm)	Levitation height of the ring±0.010, (mm)
Silver	10.00	4.000	0.800	0.000
	20.00	4.000	0.800	0.000
	30.00	4.000	0.800	0.000
	40.00	4.000	0.800	0.000
Gold	10.00	5.000	0.800	0.000
	20.00	5.000	0.800	0.000
	30.00	5.000	0.800	0.000
	40.00	5.000	0.800	0.000
Mercury	10.00	6.000	2.500	0.000
	20.00	6.000	2.500	0.000
	30.00	6.000	2.500	0.000
	40.00	6.000	2.500	0.000

Table A.13 The variable parameters for both aluminum and copper rings (needed to calculate the conductivity).

Physical parameter	Aluminum	Copper
Angular frequency of the power supply, ω, (rad/s)	377.1	377.1
Radius of the core, X, (mm)	4.000	4.000
Length of the solenoid, L±0.010, (mm)	105.0	105.0
Current in the solenoid, I± 0.001, (A)	0.780	1.700
Number of turns of the solenoid, (N)	450.0	450.0
Levitation height of the ring, Z±0.010, (mm)	About to levitate	About to levitate
Density, ρ , ($\times 10^3$, kg/m^3)	2.700	8.900
The permeability constant, μ, ($\times 10^{-3}$, Tm/A)	1.347	1.095

Table A.14 Measured data used to calculate the specific heat capacity of aluminum, when the voltage across the solenoid coil 12.3 V and the initial temperature of the ring (T_i) 25 ^{0}C.

Final temperature (T_f) ±1.000, (^{0}C)	**Current in the solenoid before insertion of the ring±0.001, (A)**	**Current in the solenoid after insertion of the ring ±0.001, (A)**	**Elapsed time ±1.000, (sec)**
25.00	0.550	0.670	0.000
29.00	0.550	0.670	27.00
31.00	0.550	0.670	45.00
35.00	0.550	0.670	68.00
37.00	0.550	0.670	73.00
39.00	0.550	0.670	80.00
42.00	0.550	0.670	109.00
42.00	0.550	0.670	120.00
42.00	0.550	0.670	150.0

Table A.15 The relation between the magnetic field B_z at the end of the solenoid with core and the current in the solenoid.

Current in the solenoid ±0.010, (A)	**Magnetic field B_z ±0.100 , (mT)**
0.085	21.00
0.110	30.00
0.160	53.00
0.290	109.0
0.370	141.0
0.420	162.0
0.480	183.0
0.590	223.0
0.640	239.0
0.770	278.0
0.800	290.0
0.870	308.0
0.930	329.0

Table A.16 The magnetization density of the core, M, over the end of the solenoid and the current in the solenoid at point on the core 0.4 cm above the upper end of the solenoid.

Magnetic field intensity H, ($\times 10^6$, A/m).	**Induced voltage (m V) ±1.000, (A)**	**Magnetization density M, ($\times 10^4$, A/m)**	**Current in the solenoid ±0.010, (A)**
4.350	33.00	2.387	2.030
5.507	38.20	4.643	2.570
6.857	39.00	16.92	3.200
7.585	46.00	18.65	3.540
7.971	47.00	20.40	3.720
9.557	51.00	22.13	4.460
11.23	53.80	23.35	5.240
12.86	56.60	24.56	6.000
14.79	59.00	25.60	6.900

Table A.17 The induced *emf* and other properties of aluminum, copper and iron rings.

Type of material	**Aluminum**	**Copper**	**Iron**
Induced voltage across the ring ±1.000 (mV)	4.000	4.000	4.000
Length of the ring ±0.010 (mm)	40.00	40.00	40.00
Thickness of the ring ± 0.010 (mm)	1.000	1.200	0.800
Radius of the ring ±0.01 (mm)	10.00	11.000	14.00
Conductivity of the ring ($\times 10^7$ S/m)	3.571	5.882	1.000

Table A.18 The current drawn by the solenoid coil and the thickness of aluminum ring, for fixed rings length of 9.5 mm, and voltage across the solenoid coil 20 V.

Solenoid current ±0.001, (A)	**Ring thickness ±0.010 ,(mm)**
0.350	0.000
0.410	1.000
0.440	2.900
0.450	4.000
0.470	7.000

Table A.19 The drawn current by the solenoid coil, and the length of copper ring, for fixed rings thickness 0.77 mm and potential difference of 20 V.

Solenoid current ± 0.010, (A)	**Ring length ± 0.010, (mm)**
2.100	0.000
2.300	10.00
2.420	20.00
2.500	30.00
2.700	80.00

Table A.20 The B_r and the corresponding radial distance from the core (r) measured at the top of the solenoid for constant solenoid current of 2 A.

r ± 0.010, (mm)	**B_r ± 0.100, (mT)**
4.000	20.00
5.000	15.00
6.000	10.00
7.000	6.000
8.000	4.000
9.000	3.000
10.00	2.500
11.00	2.000
12.00	1.000

Table A.21 The fluctuations and the systematic errors of apparatus.

Device	**fluctuation**	**systematic error**
Teslameter	5%	1.000, (mT)
Ammeter	4%	1.000,(mA)
Voltmeter	4%	1.000, (mV)
Instruments		
Caliper	0.1000 ,(mm)	
Ruler	1.000, (mm)	
Thermometer	0.500, (^{0}C)	
Hand watch	1.000, (s)	
Electronic mass balance	0.010, (g)	

Appendix B

Derivation of the magnetic field and the magnetic force on the ring

B.1 The magnetic field due to a circular current loop

Consider a current loop of radius a placed in the x y-plane and carries a current I as shown in Figure B.1.

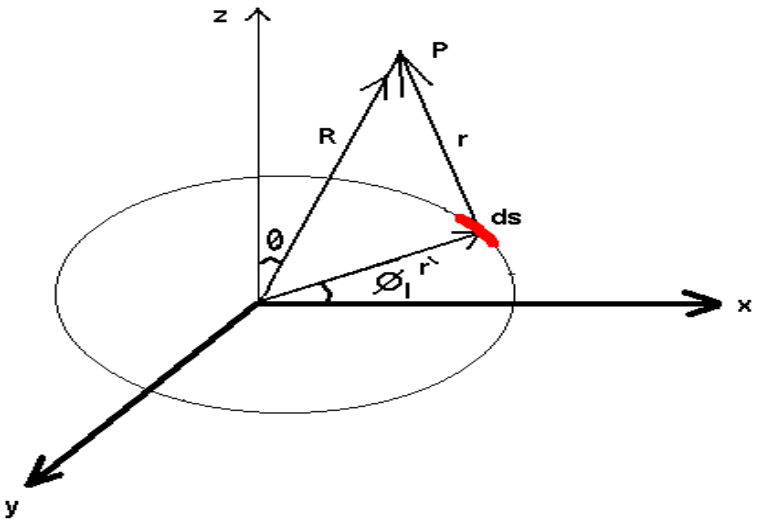

Figure B.1 The magnetic field produced by circular current loop carrying a current I at space point P.

The differential current element *Ids* located at r′ can be written as:

$$Id\vec{s} = aI(-\sin(\Phi_1)\hat{i} + \cos(\Phi_1)\,\hat{j})d\Phi \qquad \text{(B.1)}$$

The position vector of point P in spherical coordinates (R,θ,Φ_1) can be written as:

$$\vec{R} = R\sin(\theta)\cos(\Phi_1)\hat{i} + R\sin(\theta)\sin(\Phi_1)\hat{j} + R\cos(\theta)\hat{k} \tag{B.2}$$

and

$$\vec{r} = \vec{R} - \vec{r}' \tag{B.3}$$

Accordingly, the relative position vector r in equation (B.3) can be rewritten as:

$$\vec{r} = \left[R\sin n(\theta)\cos(\Phi_1) - a\cos(\Phi_1)\right]\hat{i} + \left[R\sin n(\theta)\sin(\Phi_1) - a\sin(\Phi_1)\right]\hat{j} + R\cos(\theta)\hat{k} \tag{B.4}$$

where

$$\vec{r}' = a\cos(\Phi_1)\hat{i} + a\sin(\Phi_1)\hat{j} \tag{B.5}$$

Let us now introduce the A, B and D parameters as follows:

$$\left.\begin{aligned} A &= \left[R\sin n(\theta)\cos(\Phi_1) - a\cos(\Phi_1)\right] \\ B &= \left[R\sin n(\theta)\sin(\Phi_1) - a\sin(\Phi_1)\right] \\ D &= R\cos(\theta) \end{aligned}\right\}, \tag{B.6}$$

Thus, the relative position vector can be expressed in terms of A, B, and C as:

$$\vec{r} = A\hat{i} + B\hat{j} + D\hat{k} \tag{B.7}$$

The magnitude of r can be simplified into the following expression:

$$|r| = \left[R^2 + a^2 - 2Ra\sin(\theta)\cos(\Phi_1) \right]^{1/2} \qquad \text{(B.8)}$$

The magnetic field at P produced by the current element according to Biot-Savart law is:

$$d\vec{B} = \frac{\mu_0 I}{4\pi} \frac{d\vec{s} \times \vec{r}}{r^3} \qquad \text{(B.9)}$$

By making use of equation (B.4) and performing the cross product in equation (B.9), we get

$$d\vec{B} = \frac{\mu_0 I}{4\pi} \frac{\left[\left(aD\cos(\Phi_1)\right)\hat{i} + \left(aD\sin(\Phi_1)\right)\hat{j} - \left(aB\sin(\Phi_1) + aA\cos(\Phi_1)\right)\hat{k} \right] d\Phi}{\left[R^2 + a^2 - 2Ra\sin(\theta)\cos(\Phi_1) \right]^{3/2}} \qquad (B.10)$$

Integrating equation (B.10) for a full range of Φ, we get

$$\vec{B} = \frac{\mu_0 I}{4\pi} \int_0^{2\pi} \frac{\left[\left(aD\cos(\Phi_1)\right)\hat{i} + \left(aD\sin(\Phi_1)\right)\hat{j} - \left(aB\sin(\Phi_1) + aA\cos(\Phi_1)\right)\hat{k} \right] d\Phi}{\left[R^2 + a^2 - 2Ra\sin(\theta)\cos(\Phi_1) \right]^{3/2}} \qquad (B.11)$$

Relatively speaking, the distribution of the magnetic field at P can be represented by two components as follows: The radial component B_r in the direction of the radius of the loop and the vertical component B_z in the z

direction. According to equation (B.11), the horizontal component of the magnetic field B_r is:

$$B_r = \frac{\mu_0 IaR\cos(\theta)}{4\pi} \int_0^{2\pi} \frac{\cos(\Phi)d\Phi}{\left(a^2 + R^2 - 2aR\sin(\theta)\cos(\Phi)\right)^{3/2}} \tag{B.12}$$

The vertical component of the magnetic field B at any point along the z axis is obtained by substituting equation (B.6) and $\theta = 0$ in equation (B.11) and integrating it to get:

$$B_z = \frac{\mu_0 Ia^2}{2(a^2 + z'^2)^{3/2}} \tag{B.13}$$

The expression of the magnetic field in equation (B.12) can be approximated by expanding the dominator in equation (B.8) as follows:

$$|r|^{-3} = \frac{1}{\left(a^2 + R^2\right)^{3/2}} + \frac{3aR\sin(\theta)\cos(\Phi)}{\left(a^2 + R^2\right)^{5/2}} + ------ \tag{B.14}$$

Keeping only the first two terms in equation (B.14), the truncated result can be written as:

$$\left|r^{-3}\right| = \frac{\left(a^2 + R^2\right)^2 + 3aR\sin(\theta)\cos(\Phi)}{\left(a^2 + R^2\right)^{5/2}} \tag{B.15}$$

Substituting equation (B.15) into equation (B.12), we get:

$$\vec{B} = \frac{\mu_0 I}{4\pi} \int_0^{2\pi} \frac{\left[(aD\cos(\Phi_1))\hat{i} + (aD\sin(\Phi_1))\hat{j} - (aB\sin(\Phi_1) + aA\cos(\Phi_1))\hat{k}\right]}{\left[a^2 + R^2\right]^{5/2}}$$

$$\frac{\left(\left(a^2 + R^2\right)^2 + 3aR\sin(\theta)\cos(\Phi)\right)d\Phi}{\left[a^2 + R^2\right]^{5/2}} \qquad \text{(B.16)}$$

The total magnetic field produced at P is obtained by summing all contributions from all differential current elements. The component of the magnetic field in the r direction can be written as:

$$B_r = \frac{\mu_0 I}{4\pi}\left[\int_0^{2\pi} \frac{[aD\cos(\Phi)]\left(a^2 + R^2\right)^2 d\Phi}{\left(a^2 + R^2\right)^{5/2}} + \int_0^{2\pi} \frac{3a^2 RD\sin(\theta)\cos^2(\Phi)d\Phi}{\left(a^2 + R^2\right)^{5/2}}\right] \qquad \text{(B.17)}$$

The first term is zero, since the integral of cosine angle over a complete cycle is zero. Substituting equation (B.6) into equation (B.17) and integrating the result, the B_r component becomes:

$$B_r = \frac{3\mu_0 I a^2 R^2 \sin(\theta)\cos(\theta)}{4\pi\left(a^2 + R^2\right)^{5/2}} \qquad \text{(B.18)}$$

Using the near axis approximation $(R = z')$, we get

$$B_r = \frac{3\mu_0 I a^2 R^2 \sin(\theta)\cos(\theta)}{4\pi\left(a^2 + z'^2\right)^{5/2}} \tag{B.19}$$

In order to simplify the problem, the coordinate has to be rotated in away such that the position of the point P will be located in the x-z plane. Then, the location of P in cartesian coordinates is P(x,0,z) as shown in Figure B.2.

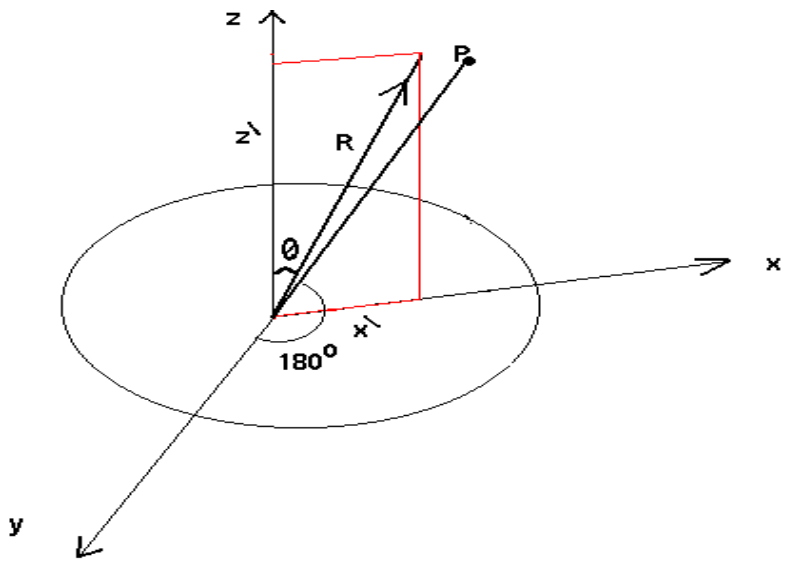

Figure B.2 Schematic representations of the magnetic field due to circular current loop carrying a current I at P(x,0,z).

Clearly, from Figure B.2, the following expressions can be written

$$\left\{\begin{array}{l} R\cos(\theta) = z' \\ R\sin(\theta) = x' \end{array}\right\} \tag{B.20}$$

Substituting the value of R cos(θ) and R sin(θ) into equation (B.19) to get:

$$B_r = \frac{3\mu_o I a^2 R^2 z' x'}{4\pi\left(a^2 + z'^2\right)^{5/2}} \qquad \text{(B.21)}$$

The total magnetic field can be written as:

$$\vec{B} = B_r \hat{r} + B_z \hat{z} \qquad \text{(B.22)}$$

Where B_r and B_z are given in equation (B.13) and equation (B.21). These components are displayed in Figure B.3.

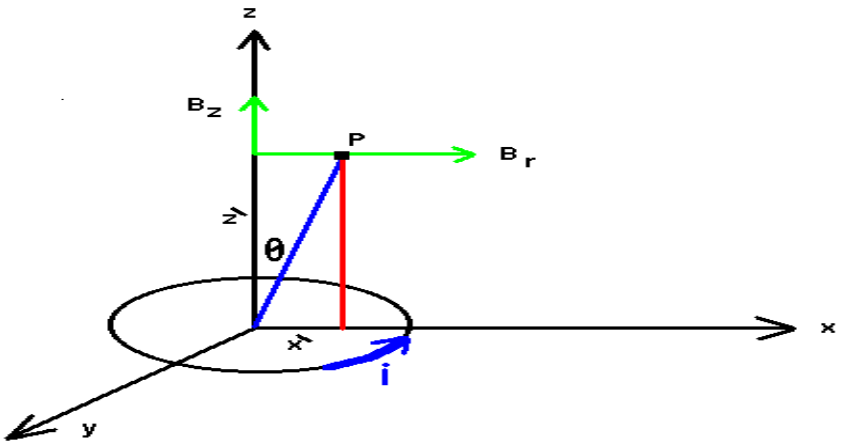

Figure B.3 Schematic representations of the two components B_z and B_r of the magnetic field B due to a circular current loop.

B.2 The magnetic field of a solenoid

Next there is a need to derive an expression for the magnetic field B produced in the solenoid at any point near the core. For this purpose consider a solenoid of length ***L*** and N turns carrying an alternating current I as:

$$I = I_0 \sin(\omega t) \tag{B.23}$$

Here I_0 is the maximum current in the solenoid or the root-mean-squared (rms) value, I_{rms} of the current, ω is the angular frequency of the current source and t is the time.

The current I will produce a magnetic field B inside the solenoid. The magnetic field at any point near the core of the solenoid can be expressed as in equation (B.22) (Summner and Thakkrar, 1972). In this case, B_z and B_r are the vertical and the radial components of the magnetic field at any point P above the upper end of the solenoid as shown in Figure B.4. In the following subsections, complete derivations of both components were separately made.

B.2. 1 Derivation of B_z for the solenoid

Need to find an expression for B_z at any point P above the upper end of the solenoid at a distance z as shown in Figure B.4. Applying equation (B.29) to a very thin section of a solenoid having a number of turns N, with d_z radius a, a total current *I*Ndz, core permeability μ, and using equation (B.13) to get:

$$dB_z = \frac{\mu NI}{2L}\frac{a^2}{(a^2+z'^2)^{3/2}}dz' \qquad \text{(B.24)}$$

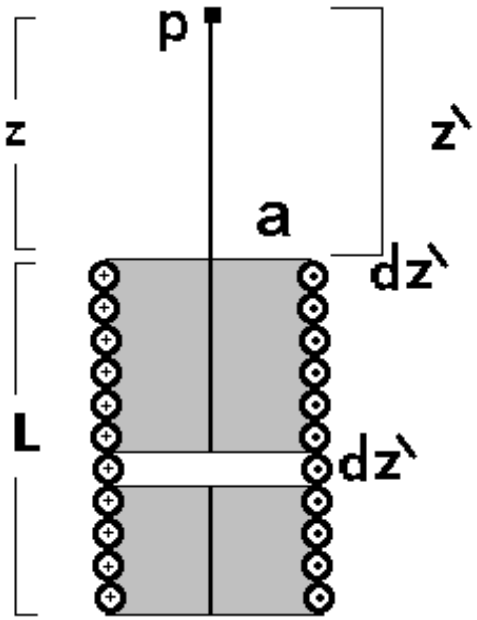

Figure B.4 Schematic representations showing a solenoid of N turns and the point P along solenoid axis where the magnetic field should be calculated.

Integrating equation (B.24) from z to (z+***L***) to obtain the following results for B_z

$$B_z = \int_z^{z+L} \frac{\mu NI}{2L} \frac{a^2}{\left(a^2 + z'^2\right)^{3/2}} dz' = \frac{\mu NI}{2L} \frac{z'}{\sqrt{\left(a^2 + z'^2\right)}} \Bigg]_z^{z+L} \tag{B.25}$$

The final result can be written as:

$$B_z = \frac{\mu NI}{2L} \left\{ \frac{z+L}{\sqrt{\left(a^2 + (z+L)^2\right)}} - \frac{z}{\sqrt{\left(a^2 + z^2\right)}} \right\} \tag{B.26}$$

Introducing the *y* and *f* parameters as:

$$y = \sqrt{\left(a^2 + z^2\right)} \tag{B.27}$$

and

$$f = \sqrt{\left(a^2 + (z+L)^2\right)} \tag{B.28}$$

Substituting equations (B.27) and equation (B.28) into equation (B.26) to get:

$$B_z = \frac{\mu NI}{2L} \left(\frac{(z+L)}{f} - \frac{z}{y} \right) \tag{B.29}$$

Inserting equation (B.23) into equation (B.29) it becomes:

$$B_z = \frac{\mu\ N_0}{2L} \left[\frac{(z+L)}{f} - \frac{z}{y} \right] \sin(\omega t) \tag{B.30}$$

Now, the maximum vertical magnetic field, B_{z0}, at point along the axis of the solenoid is:

$$B_{z_0} = \frac{\mu\ NI_0}{2L}\left[\frac{(z+L)}{f} - \frac{z}{y}\right] \tag{B.31}$$

Thus, equation (B.31) can be rewritten as:

$$B_z = B_{z0}\sin(\omega t) \tag{B.32}$$

Hence, the magnetic field at any point z is sinusoidal.

B.2.2 The radial component of the field (B_r)

This component is directed parallel to the radius of the solenoid along the r- direction as shown in Figure B.4. The derivation of B_r at any point P(r, z) on the axis of a circular current loop may be written as in equation (B.21) (Simpson *et al*., 2001). Following the same procedures previously used in section 2.2.4.1 and applying equation (B.21) to a thin section of a solenoid of width *dż* having a total current of *I* N*dż* and radius a, one may write for B_r:

$$dB_r = \frac{3Na^2\mu_0 Irz'}{4\left(a^2 + z'^2\right)^{5/2}}dz' \tag{B.33}$$

Integrating equation (B.33) to get:

$$B_r = \int_{z}^{z+L} \frac{3Na^2\mu_0 Irz'}{4\left(a^2 + z'^2\right)^{5/2}} dz' \qquad \text{(B.34)}$$

It easy to show that integration of equation (B.34) will produce the following expression:

$$B_r = \frac{Na^2\mu_0 Ir}{4}\left[\frac{f^3 - y^3}{f^3 y^3}\right] \qquad \text{(B.35)}$$

Where *f* and *y* are defined by equation (B.27) and equation (B.28).

By making use of equation (B.23), equation (B.35) can be rewritten as:

$$B_r = \frac{Na^2\mu_0 I_0 r}{4}\left[\frac{f^3 - y^3}{f^3 y^3}\right]\sin(\omega t) = \mathrm{B}_{r0}\sin(\omega\, \mathrm{t}) \qquad \text{(B.36)}$$

where $B_{r_o} = \frac{Na^2\mu_o I_o r}{4}\left[\frac{f^3 - y^3}{f^3 y^3}\right]$ is amplitude of B_r, which is defined as the maximum horizontal magnetic field at any point along the radial axis of the solenoid core. Equations (B.32) and (B.36) represent the vertical and the horizontal components of the magnetic field (B_{ext} at any point along the axis of the solenoid in air (Portis, 1978). The magnetic field inside the core, B_{in}, can be written as:

$$B_{in} = B_{ext} + \mu_0 M = B_{ext} + C_3 \tag{B.37}$$

Where C_3 is constant equal to μ_o M, M is the magnetization density of the metal core, and μ_o is the permeability of the air. The magnetic field inside the core is B_{in} while the external field resulting from the solenoid is B_{ext}. Moreover, the vertical component of the field inside the core is $B_{z\,in}$ and the radial component of the field inside the core is $B_{r\,in}$. Since the field lines that induce B_z are practically inside the metal and the B_r is acting on the ring is far from the core (in air) equation (B.35) can be rewritten as:

$$B_{z\ in} = \frac{\mu_0 I_0}{2L}\left[\frac{z}{y} - \frac{(z+L)}{f}\right] + C_3 \tag{B.38}$$

and

$$B_{r\ in} = \frac{Na^2\mu_0 Ir}{4}\left[\frac{f^3 - y^3}{f^3 y^3}\right] + C_3 \text{ , for } 0 \le r \le a \tag{B.39}$$

Finally,

$$B_r = \frac{Na^2\mu_0 Ir}{4}\left[\frac{f^3 - y^3}{f^3 y^3}\right], \quad \text{for } r > a \tag{B.40}$$

B.3 Induced *emf* across the floating ring

In this section we need to establish a relation between an eddies current produced in the non-magnetic materials placed in the vicinity of an alternating magnetic field and its magnetic and electric properties as well as to examine some characteristics of the material. Let a non-magnetic metal ring is inserted in the metal core of a solenoid and allowing an alternating current to pass through. An *emf* is then produced across the ring as a result of the electromagnetic induction of the z component of the alternating magnetic field B_z and an eddy current (*dI*) flowing through (i.e. circulate) the ring and forcing it to levitate, as a result of the repulsive force dF between the magnetic field of the solenoid and the opposing field resulting from the eddy current passing through the ring. In deriving an expression for the *emf*, we shall first derive an expression for open circuit ring (one turn). Before doing that, it is of great importance to make a list of variables to be appeared in the equations and formulae. Thus, the most well known variables introduced for the ring (see Figure B.5) are listed below:

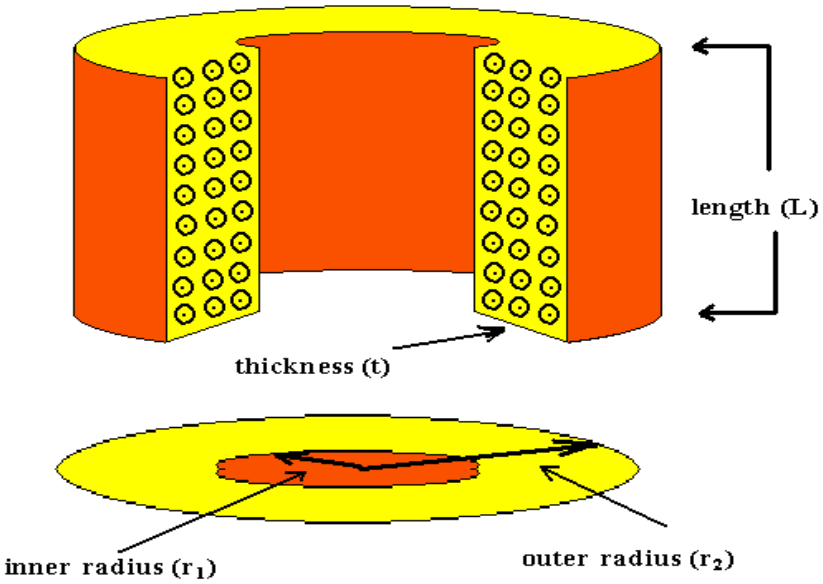

Figure B.5 Schematic representations of the ring dimensions and the flow of the eddy current through it.

A is the cross sectional area of the ring.

R is the electrical resistance between two points on the ring (see Figure B.5 and Figure B.6).

r_1 is the inner radius of the ring,

r_2 is the outer radius of the ring,

r is the average (mean) radius, $= \frac{r_1 + r_2}{2}$

σ is the conductivity of the metal ring,

l is the circumference of the ring,

t is the thickness of the ring,

L is the ring length,

I is the eddy current induced in the ring,

m is the ring mass,

ρ is the ring material density,

emf is the induced voltage across the terminates of the open circuit ring,

x is the radius of the core.

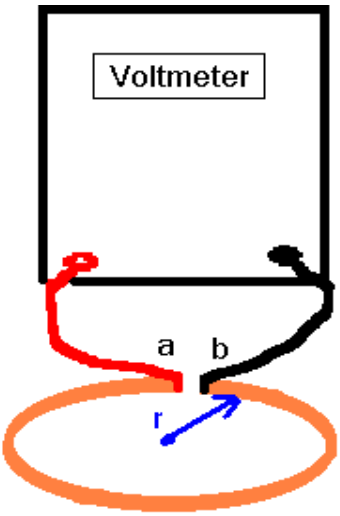

Figure B.6 Schematic representations showing measurement arrangement of the induced *emf* across the ring between two points.

Let us consider the case when the ring is inserted coaxially with the core passing through a solenoid. In such case, the magnetic flux through the ring Φ and the *emf* is the potential difference produced across it as shown in Figure B.5 and Figure B.6.

The magnetic flux linkage through the ring is given by (Portis, 1978):

$$\Phi = \vec{B}.\vec{A} \qquad \text{(B.41)}$$

Where B and A are shown in Figure B.7.

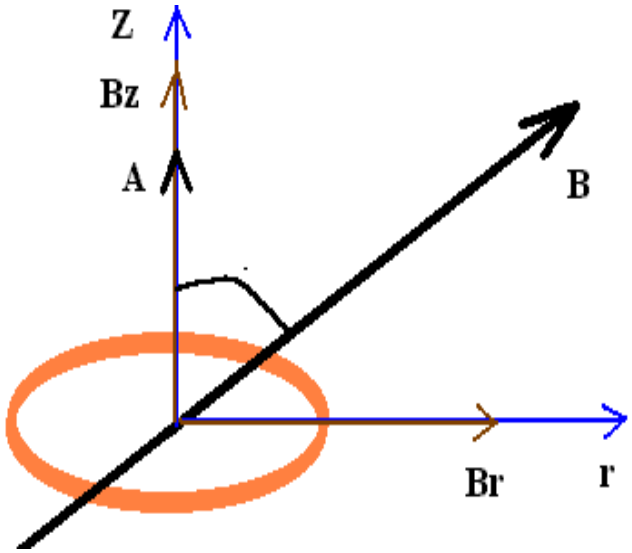

Figure B.7 The magnetic field B through copper ring of cross sectional area A.

Using equation (B.22) and $\vec{A} = A\hat{z}$, equation (B.41) will be rewritten as:

$$\Phi = (B_r \hat{r} + B_Z \hat{z}).\vec{A} = B_Z A = B_{zo} \sin(\omega t) \qquad \text{(B.42)}$$

where $B_z = B_{zo}\sin(\omega t)$ has been used in equation (B.42). By making use of Faraday's law of induction and equation (B.42), the potential is defined as (Halliday *et al.*, 1986):

$$|emf| = \left| -\mathrm{n}\frac{\mathrm{d}\Phi}{\mathrm{dt}} \right| = \mathrm{n}\omega\,\mathrm{B}_{z0}\mathrm{A}\cos(\omega\,\mathrm{t}) = \mathrm{e}mf_{\max}\cos(\omega\,\mathrm{t}) \qquad \text{(B.43)}$$

where

$$\mathrm{e}mf_{\max} == \mathrm{n}\,\omega\,\mathrm{B}_{z0}\,\mathrm{A} \qquad \text{(B.44)}$$

Substituting $A = \pi x^2$ in equation (B.44) to get:

$$\mathrm{e}mf_{\max} = \mathrm{n}\,\omega\,\mathrm{B}_{z0}\mathrm{A} = \omega\,\mathrm{B}_{z0}\,\pi\,\mathrm{x}^2 \qquad \text{(B.45)}$$

In this study, the area, A, in which flux is enters is constant. This is because the effective area assigned for the flux lines to pass through is that of the cross sectional area of the core itself. One may argue this from the fact that most of the field lines which cause the induction to the ring is lies through the core, thus the cross sectional area A is taken to be the area of a ring of radius x.

B.4 The eddy current produced in a metal ring

When the ring is treated as a short circuit, the potential difference produced across the ring, as a result of the induced eddy current, *dI*, in the internal resistance R which flows (i.e. circulate in the ring) in a direction perpendicular to the cross section area (t *dz*). If *l* is the circumference of the ring as shown in Figure B.6, then by Ohms law the *emf* is given as (Halliday *et al.*, 1981):

$$emf_{\max} = dI\ \mathrm{R} \tag{B.46}$$

where R is the resistance of the ring. Using the basic definitions, it is easily to write the following expressions:

$$R = \frac{l}{\sigma t dz} \tag{B.47}$$

By making use of equation (B.46) and equation (B.47), the current element is

$$dI = \frac{emf_{\max}\,\sigma\ \mathrm{t dz}}{l} \tag{B.48}$$

Substituting equation (B.45) into equation (B.48) to get

$$dI = \frac{\omega\ \mathrm{t\ A\ B_{zo}}\sigma\ \mathrm{dz}}{l} \tag{B.49}$$

Integrating equation (B.49) from z_1 to z_2 to get the total current. Thus,

$$I = \frac{\omega\ \mathrm{t\ A\ B_{z0}}\sigma\ \mathrm{L}}{l} \tag{B.50}$$

where L is the length of the ring $L=(z_1-z_2)$.

B.5 Derivation of the levitating magnetic force on the ring

The force on a current element *I*d*l* as inferred from experiments on closed current loops (see Figure B.8), (Kip , 1969) is:

$$d\vec{F}=id\vec{l}\times\vec{B} \qquad \text{(B.51)}$$

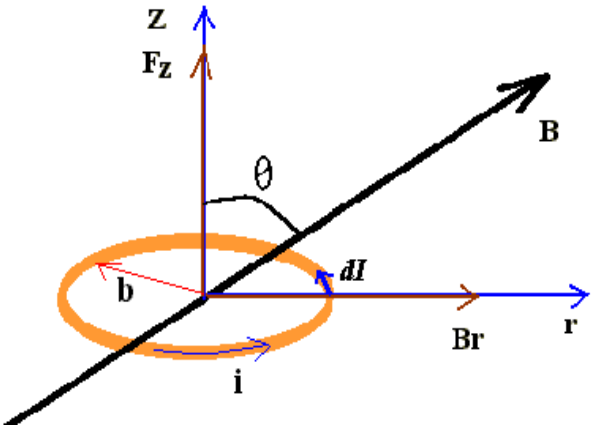

Figure B.8 The vertical force on the ring F_z.

Because there are two component of magnetic field B_r and B_z, the ring is subjected to two different forces; the first one arises from the interaction of B_r with the induced field from the eddy current in the ring. Clearly this force is F_z, component of F along z-direction. The other force is the result of interaction of B_z with the induced field from the eddy current in the ring.

This force is acting along r direction and representing the radial component F_r.

Using equation (B.22) and $d\vec{l} = dl\hat{\theta}$ into equation (B.51), the result can be written as:

$$d\vec{F} = \left[idl\hat{\theta} \times B_r\hat{r}\right] + \left[idl\hat{\theta} \times B_z\hat{z}\right] = lB_z dI\hat{r} + lB_r dI\hat{z}$$
$$= dF_r\hat{r} + dF_z\hat{z} \qquad \text{(B.52)}$$

The force components $d\vec{F}_r$ and $d\vec{F}_z$ represent the radial and the vertical components, respectively. The resultant of F_r is zero. This is because of symmetry (see Figure B.9) (Summner and Thakkrar, 1979).

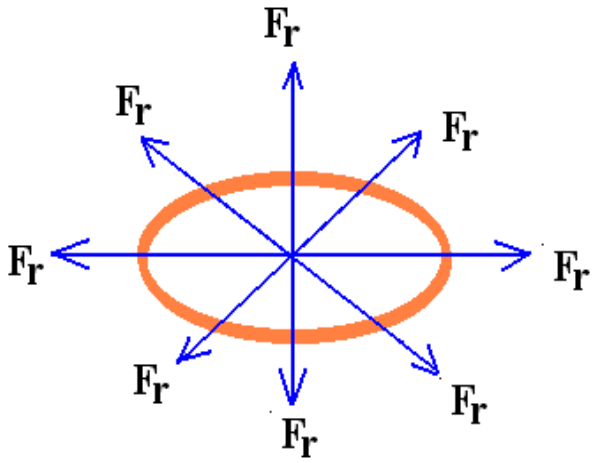

Figure B.9 Schematic representations showing the resultant radial forces on the ring F_r.

Therefore, the z-component of the force $d\vec{F}_z$, is needed to be discussed in more details. When *i* in these expressions is replaced by *dI*, the force component $d\vec{F}_z$ can be rewritten as:

$$d\vec{F}_z = lB_r dI\hat{z} \tag{B.53}$$

Substituting the expression of *dI* from equation (B.49) into equation (B.53) we get:

$$dF_z = \left[wtAB_r B_z\right]dz \tag{B.54}$$

Equation (B.54) represents the magnetic force acting on a small portion of the ring having a length *dz*, or a circular loop of one turn. In order to find the force on a ring of length L, we integrate equation (B.54). Thus,

$$F_z = \int_{z_1}^{z_2}\left[\omega tA\sigma\frac{N^2a^2{\mu_0}^2i^2r}{8L}\left[\frac{z}{y}-\frac{(z+L)}{f}\right]\left[\frac{f^3-y^3}{f^3y^3}\right]\right]dz \tag{B.55}$$

where *f* and *y* are given by equation (B.27) and equation (B.28)

B.6 The relation between the levitation height of the ring and other variables at equilibrium

The ring levitates a few centimeters (Ford and Sullivan, 1991) before it settles in position under the effect of zero resultant force. Let us consider a ring of length $L = z_2 - z_1$, such that z_1 and z_2 represent the distances of the

lower and the upper ends of the ring measured from the upper top of the solenoid as shown in Figure B.10.

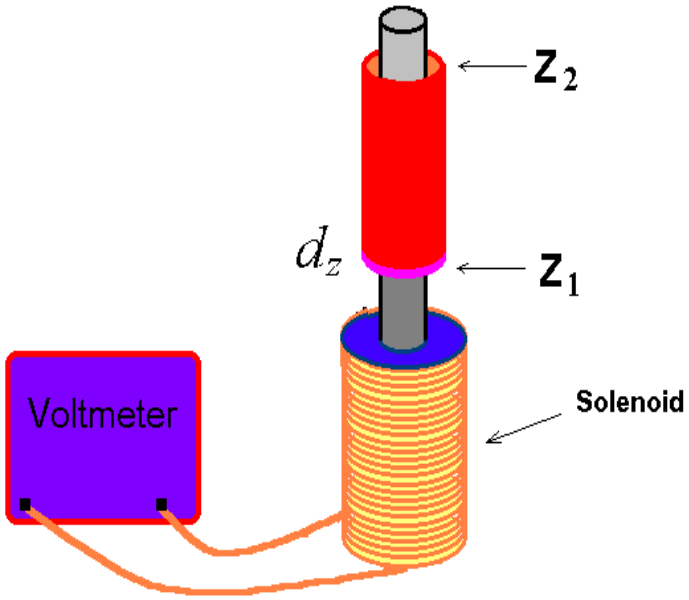

Figure B.10 Elevation of copper ring above a solenoid coil carrying an AC current.

Consider a thin cross sectional part of a ring of mass dm and length *dz*, in which an eddy current *dI* is passing through. Then at the equilibrium, the weight, w, of the ring is equal to the force pushing the ring upward, F_z.

Therefore,

$$dw = \rho\, ltgdz = dF_z \tag{B.56}$$

By equating equation (B.56) with equation (B.54), the following equation is obtained:

$$\rho\, l\, t\, gdz = \left[\omega\, t\, A\sigma nnB_r B_z\right]dz \tag{B.57}$$

Integrating both sides to get,

$$\frac{\rho l.gL}{wA\sigma} = \int_{z_1}^{z_2} B_r B_z dz \qquad \text{(B.58)}$$

As a special case, if the ring is assumed to be so small, then B_rB_z can be taken to be constants over an infinitesimal segment of its length. Thus, integrating the right-hand side (R.H.S) of equation (B.58) to give:

$$\int_{z_1}^{z_2} B_r B_z dz = B_r B_z (z_2 - z_1) = B_r B_z L \qquad \text{(B.59)}$$

Substituting equation (B.59) into equation (B.57), the following equation is obtained:

$$B_r B_z L = \frac{\rho\, l.gL}{\omega\, A\sigma} \qquad \text{(B.60)}$$

By making use of $l = 2\pi r$ and $A = \pi x^2$, equation (B.60) then takes the following form:

$$B_r B_z = \frac{2g\rho\, r}{\omega\sigma\, x^2} = \text{constant} \qquad \text{(B.61)}$$

where A is the cross sectional area of the core.

Accordingly, the momentarily increase of the voltage is followed by an increase of the current in the solenoid. Thus, the force on the ring will be increased and the ring levitates upward in order to decrease the force and to reach the point at which the force is the same as it was initially (Sumner and Thakkrar, 1979). Substituting equation (B.38) and equation (B.40) into equation (B.61) to get:

$$\left(\frac{\mu_0 N i_0}{2L}\left[\frac{(z+L)}{f}-\frac{z}{y}\right]+C_3\right)\left(\frac{Na^2\mu_0 i_0 r}{4}\left[\frac{f^3-y^3}{f^3y^3}\right]\right)=\frac{2\rho rg}{\omega x^2\sigma} \qquad \text{(B.62)}$$

Solving for ρ to get:

$$\rho=\frac{\omega\sigma x^2}{2g}\left(\frac{\mu_0 N i_0}{2L}\left[\frac{(z+L)}{f}-\frac{z}{y}\right]+C_3\right)\left(\frac{Na^2\mu_0 i_0}{4}\left[\frac{f^3-y^3}{f^3y^3}\right]\right) \qquad \text{(B.63)}$$

Moreover, solving for σ, to get

$$\sigma=\frac{\rho}{\frac{\omega x^2}{2g}\left(\frac{\mu_0 N i_0}{2L}\left[\frac{(z+L)}{f}-\frac{z}{y}\right]+C_3\right)\left(\frac{Na^2\mu_0 i_0}{4}\left[\frac{f^3-y^3}{f^3y^3}\right]\right)} \qquad \text{(B.64)}$$

The parameters in equation (B.63) and equation (B.64) are the corner stone of the theoretical calculations.

REFERENCES

Aiello, G., Alfonzetti, S. 2000. Finite element computation of axis symmetric eddy current in an infinite domain. *The International Journal*. **19**, pp: 167-172.

Auld, B. A., Moulder, J. C. 1998. Review of advances in Quantitative Eddy Current Nondestructive Evaluation. *J. Nondest. Eval*. **18**, pp: 3-5.

Avrin, F. W. 2000. Eddy current measurements with magneto-resistive Sensor. *Proceedings of SPI***. 3994,** pp: 29-36.

Barth, M. 2000. Electromagnetic induction rediscovered using original texts. *Sience and Education*. **9**, pp: 375-3387.

Bishop, J. E. L. 2001. Eddy current loss calculation for skew, bracket and wedge domain walls as in (110) (001) SiFe lamination. *Elect. J*. **3**, pp: 139-141.

Blitz, J., Alagoa, K. D. 1985. Eddy-current testing of woods metal models for inclined cracks. *Ndt International*. **18**, pp: 269-273.

Cimatti, G. 2003. The Eddy Current problem with temperature dependent Permeability. *Elect. J. Diff. Eqns*. **2003**, pp: 1-5.

Deene, Y. D., Wagter, C. D., Neve, W. D., Achten, E. 1999. Artefacts in multi precision gel dosimetry. Analysis and compensation of eddy currents. *Phys. Med. Biol*. **45**, pp: 1807-1823.

Fleming, J.A. 1970. The royal institution library of science. *Phyi. Ca Sciences*. **4,** pp: 72-90.

Ford, P.J., Sullivan, R. A. l. 1991. The jumping ring experiment revisited. *School of Phys.*. pp: 380-382.

Ford, P. J., Sullivan, R. A. L., Pilkington., Rowe, M. 1992. *Physics Experiments and S Chomet*. London: Newman-Hemisphere, pp: 308-385.

Freeman, E. M., Lother, D.A. 1989. An open boundary technique for symmetric and three dimensional magnetic and electric field problems. *IEEE Trans. Mag*. **25**, pp: 4135-4137.

Freeman, E. M., Bland, T.G. 1976. Equivalent circuit of concentric cylindrical conductors in an axial alternating magnetic field. *IEEE Trans. Mag*. pp: 149-152.

Freeman, E.M., Lowther, D.A., Laithwaite, E.R. 1975. Scale model linear induction motors. *Proc .IEE*, pp: 7721-726.4.

Freeman, E.M. 1992. *The Magnet User Guide*. *Montreal: Infolytica Corp*, pp: 300-307

Gros, X. E. 1995. An eddy current approach to the detection of damage caused by low -energy impacts on carbon fiber reinforced Materials and Design. *Material and design*. **16**, pp: 167-173.

Hallidy, D., Resnick, R., Walker, J. 2001. *Fundamental of Physics*. 6^{th} *ed* , New York : John Wiley, pp: 608-617.

Hall, J. 1997. Force on the jumping ring. *The Physics Teacher*. **35**, pp: 80 82.

Hammond, P. 1971. *Applied Electromagnetism*. Wheaton: Exeter, pp: 400-412.

Hoffmann, B., Houbertz, R., Hurtmann, U. 1997. Eddy current Microscopy. *Appl. Phys*. A. **66**, pp: 409-413.

Huang, D.R. 2003. Study of eddy current power loss from outer winding coils of a magnetic position sensor. *J. Mag. Mat*. **209**, pp: 201-204.

Kip, A. 1969. *Fundamentals of electricity and magnetism*. New York: McGraw Hill, pp: 238-361.

Koch, M., Norris, D. 2000. An assessment of eddy current sensitivity and correction in single-shot diffusion-weighted imaging. *Phys. Med*. **45**, pp: 3821-3832.

Lebrun, B., Jayet, Y., and Baboux, J. C. 1997. Pulsed eddy current signal Analysis. *NDT & E International*. **30**, pp: 163-170.

Page, L., Adams, N. L. 1987. *Principles of Electricity*. New York: Van Nostrand, pp: 400-430.

Portis, A. 1978. *Electromagnetic Fields*. New York: John Wiley and Sons. pp: 500-617.

Rao, B. P. C, C., and Babu Rao, T. J. B. 1996. Simulation of eddy current signals from multiple defects. *NDT & E International*. **29,** pp: 269-2273.

Restivo, M. T. 1996. A case study of induced eddy currents. *Sensor and Actuators*. A. **51**, pp: 203-210.

Sikora, R., Gratkowski, S., Komorowski. 2000. Eddy current based on determining of conductivity and permittivity. *The international Journal*. **19**, pp: 352-356.

Simpson, J., Lane, J., Lmmer, C., Youngquist. 2001. Simple Analytical Expressions for the Magnetic field of a Circular Current loop. *NASA.* **10**, pp: 1-6.

Summner, D. J., Thakkrar, A, K. 1972. Experiments With a 'jumping ring ' apparatus. *Physics Department Makerere University Kampal Uganda,* **C 4**, pp: 238-242.

Szczyglowski, J. 2000. Influence of eddy currents on magnetic hysteresis loops in soft magnetic materials. *Journal of Magnetism and Magnetic Materials*, pp: 97-102.

Taylor, C. A. 1988. The Art and Science of lecture Demonstrations. *Bristol: Adman Hilger*, pp: 212-250.

Thompson, N. 1990. Thinking like a physicist. *New York: Adam hailer*, pp: 106-107.

Thong, J .T .L., Fenglei, L. 2002. Eddy current compensation for magnetic electron, Lenses. *Sci. Techno*. **7**, pp: 1583-1590.

William, A. F. 2000. Eddy current measurements with magneto -resistive sensors, *Proceeding of SPIE*. **3994**, pp: 29-36.